JAMES | Journal of Advances in Modeling Earth Systems

RESEARCH ARTICLE
10.1029/2025MS005459

mloz: A Highly Efficient Machine Learning-Based Ozone Parameterization for Climate Sensitivity Simulations

Yiling Ma[1], Nathan Luke Abraham[2,3], Stefan Versick[1], Roland Ruhnke[1], Andrea Schneidereit[4], Ulrike Niemeier[5], Felix Back[6], Peter Braesicke[4], and Peer Nowack[1,6]

[1]Institute of Meteorology and Climate Research Atmospheric Trace Gases and Remote Sensing, Karlsruhe Institute of Technology (KIT), Eggenstein-Leopoldshafen, Germany, [2]Yusuf Hamied Department of Chemistry, University of Cambridge, Cambridge, UK, [3]National Centre for Atmospheric Science, Leeds, UK, [4]Deutscher Wetterdienst, Offenbach am Main, Germany, [5]Max Planck Institute for Meteorology, Hamburg, Germany, [6]Institute of Theoretical Informatics, Karlsruhe Institute of Technology (KIT), Karlsruhe, Germany

Abstract Atmospheric ozone is a crucial absorber of solar radiation and an important greenhouse gas. However, most climate models participating in the Coupled Model Intercomparison Project (CMIP) still lack an interactive representation of ozone due to the high computational costs of atmospheric chemistry schemes. Here, we introduce a machine learning (ML) parameterization (mloz) to interactively model daily ozone variability and trends across the troposphere and stratosphere in standard climate sensitivity simulations, including two-way interactions of ozone with the Quasi-Biennial Oscillation. We demonstrate its high fidelity on decadal timescales and its flexible use online across two different climate models—the UK Earth System Model (UKESM) and the German ICOsahedral Nonhydrostatic (ICON) model. With atmospheric temperature profile information as the only input, mloz produces stable ozone predictions ∼31 times faster than the chemistry scheme in UKESM, contributing less than 4% of the respective total climate model runtimes. In particular, we also demonstrate its transferability to different climate models without chemistry schemes by transferring the parameterization from UKESM to ICON. This highlights mloz's potential for widespread adoption in CMIP-level climate models that lack interactive chemistry for future climate change assessments, particularly when focusing on climate sensitivity simulations, where ozone trends and variability are known to significantly modulate atmospheric feedback processes.

Plain Language Summary Ozone plays an important role in the climate system by acting as a greenhouse gas and by absorbing solar radiation, which ultimately affects atmospheric temperatures and circulation patterns from the stratosphere down to Earth's surface. However, most climate models used in major international assessments still rely on fixed climatological ozone fields that cannot respond to changing conditions within climate change simulations. This is mainly because simulating ozone interactively requires complex chemistry and transport calculations, which are highly computationally expensive. We here present mloz—the first fully interactive machine learning parameterization to represent ozone variability and trends in climate models. Using temperature profiles, mloz predicts daily ozone concentrations across the atmosphere and captures ozone-climate feedback under changing climate conditions at almost no extra computational cost. We tested mloz in two major climate models (UK Earth System Model [UKESM] and ICOsahedral Nonhydrostatic [ICON]) and found it works reliably in long simulations. Importantly, mloz trained on UKESM data also performed well in ICON, showing it can be transferred across different models. This approach allows climate models that lack atmospheric chemistry schemes to include a fast and interactive ozone representation, supporting broader use of interactive chemistry in Earth system modeling and helping policymakers to better understand how climate may evolve.

Key Points:

- mloz is introduced and implemented to interactively model daily ozone variability and trends in standard climate sensitivity simulations
- mloz produces accurate three-dimensional ozone fields in multi-decadal simulations at hardly any added computational cost
- The parameterization is demonstrated to be transferable across climate models by successful tests in ICOsahedral Nonhydrostatic after training on UK Earth System Model data

Supporting Information:

Supporting Information may be found in the online version of this article.

Correspondence to:

Y. Ma,
yiling.ma@kit.edu

Citation:

Ma, Y., Abraham, N. L., Versick, S., Ruhnke, R., Schneidereit, A., Niemeier, U., et al. (2026). mloz: A highly efficient machine learning-based ozone parameterization for climate sensitivity simulations. *Journal of Advances in Modeling Earth Systems*, *18*, e2025MS005459. https://doi.org/10.1029/2025MS005459

Received 4 SEP 2025
Accepted 9 MAR 2026

Author Contributions:

Conceptualization: Yiling Ma, Peter Braesicke, Peer Nowack
Data curation: Yiling Ma, Nathan Luke Abraham
Formal analysis: Yiling Ma, Peer Nowack
Funding acquisition: Peter Braesicke, Peer Nowack
Investigation: Yiling Ma

1. Introduction

Atmospheric ozone plays multiple vital roles in the Earth system and has significant impacts on human health. Most ozone is located in the stratosphere, forming the ozone layer, where it absorbs highly harmful solar ultraviolet (UV) radiation, thus protecting life on Earth (Garny & Hendon, 2022). In contrast, ozone in the troposphere acts as an air pollutant that exaggerates, among others, respiratory diseases and causes plant damage (Donzelli & Suarez-Varela, 2024). Ozone is also an important greenhouse gas (GHG) and its historical increases in the troposphere have already led to substantial radiative forcing (Garny & Hendon, 2022; Szopa et al., 2021).

Methodology: Yiling Ma, Nathan Luke Abraham, Stefan Versick, Roland Ruhnke, Peter Braesicke, Peer Nowack
Project administration: Roland Ruhnke, Peter Braesicke, Peer Nowack
Resources: Nathan Luke Abraham, Roland Ruhnke, Peter Braesicke, Peer Nowack
Software: Yiling Ma, Nathan Luke Abraham, Stefan Versick, Roland Ruhnke, Andrea Schneidereit, Ulrike Niemeier, Felix Back
Supervision: Peter Braesicke, Peer Nowack
Validation: Yiling Ma, Peer Nowack
Visualization: Yiling Ma
Writing – original draft: Yiling Ma
Writing – review & editing: Yiling Ma, Nathan Luke Abraham, Stefan Versick, Roland Ruhnke, Andrea Schneidereit, Ulrike Niemeier, Peter Braesicke, Peer Nowack

Moreover, the feedback of tropospheric and stratospheric ozone plays an important role in modulating surface warming and the atmospheric dynamics response to GHGs increases (Chiodo & Polvani, 2019; Dietmüller et al., 2014; Jonsson et al., 2004; Muthers et al., 2014; Nowack et al., 2015).

The main mechanisms governing ozone formation and loss are distinct between the stratosphere and the troposphere (Monks et al., 2015; Solomon, 1999). In the stratosphere, ozone concentrations are primarily controlled by photochemical reactions following the Chapman cycle (Chapman, 1930). These are modulated by catalytic ozone loss cycles, in particular those involving hydrogen oxides, nitrogen oxides (NO_x), and halogen radicals (Lary, 1997). Ozone loss through halogen species has been substantially enhanced by anthropogenic emissions of halogenated ozone-depleting substances, which has led to the formation of Antarctic ozone holes (Garny & Hendon, 2022). In addition to chemistry, dynamical processes—particularly stratospheric transport as part of the Brewer-Dobson Circulation (BDC)—play a crucial role in shaping ozone distributions, especially in the lower stratosphere where ozone lifetimes are longer (Plumb, 2002). Ozone variability is also influenced by natural climate variability such as the El Niño–Southern Oscillation (ENSO) (Benito-Barca et al., 2022), the Quasi-Biennial Oscillation (QBO) (Zawodny & McCormick, 1991), volcanic eruptions (Solomon et al., 2016), and solar activity (Haigh, 1994). Looking ahead, future stratospheric ozone is projected to evolve associated with GHG emission trajectories (Keeble et al., 2021), as GHG forcings will modulate ozone concentrations through their effects on atmospheric transport, background environmental conditions (e.g., temperature and humidity), and photolysis rates (Fu et al., 2019; Meul et al., 2014; Molina & Rowland, 1974). In particular, background temperature changes induce ozone anomalies via the temperature dependency of photochemical and catalytic reactions (Hocke & Sauvageat, 2023). In addition, some greenhouse gases act as chemically active constituents that (in)directly influence ozone. For example, increases in N_2O emissions enhance stratospheric NO_x production and thereby strengthen NO_x-driven catalytic ozone loss (Ravishankara et al., 2009). Tropospheric ozone, in turn, is primarily controlled by pre-cursor emissions—in particular of volatile organic compounds in the presence of NO_x—and subsequent chemical production and loss cycles, as well as dry deposition at the surface, while also being subject to long-range transport (Lu et al., 2019). Therefore, an explicit representation of ozone requires to resolve many processes governing ozone variations, involving radiative, dynamical, and chemical coupling between ozone and the climate system on various timescales.

In addition to being affected by background temperature conditions, ozone in turn leaves a characteristic imprint on the atmospheric temperature profile. By absorbing solar energy for photolysis, ozone and its production process heats up the upper stratosphere by more than 20 K (Matsumi & Kawasaki, 2003). Its short-wave and long-wave radiative heating is substantial throughout the atmosphere and ultimately also affects surface temperatures (Garny & Hendon, 2022), with the relative importance of short-wave and long-wave ozone forcing depending strongly on latitude and altitude. Since climate change is expected to substantially affect future ozone concentrations, the subsequent effects on radiation lead to an important chemistry-climate feedback (Wang et al., 2025). Ozone changes have been demonstrated to play a key role in modulating projected climate responses—from stratospheric cooling to surface warming (Chiodo & Polvani, 2019; Dietmüller et al., 2014; Muthers et al., 2014). The stratosphere responds to increasing CO_2 with cooling. This cooling enhances ozone in the mid–upper stratosphere due to the temperature dependence of catalytic ozone loss cycles (Haigh & Pyle, 1982; Jonsson et al., 2004; Meul et al., 2014; Muthers et al., 2014). The resulting ozone increase absorbs more solar radiation at higher altitudes and partially offsets stratospheric cooling in this region (Wang et al., 2025). Conversely, ozone in the lower tropical stratosphere is primarily controlled by dynamical rather than photochemical processes and is projected to decline due to an accelerated BDC and reduced ozone production caused by a thicker overhead ozone column (Meul et al., 2014). This decline further amplifies cooling in the lower stratosphere (Jonsson et al., 2004). Previous studies indicate that neglecting stratospheric ozone radiative feedback leads to an overestimation of cooling by 5–10K in the upper stratosphere and an underestimation by 2–3K in the lower stratosphere in $4\times CO_2$ simulations (Dacie et al., 2019; Garny & Hendon, 2022). Stratospheric to upper-tropospheric ozone–climate feedback can reduce surface warming by up to 20% under $4\times CO_2$ (Nowack et al., 2015; Nowack, Abraham, et al., 2018), although the uncertainty is significant across climate models since many processes are involved and relatively few climate models include a fully resolved chemistry scheme (Dietmüller et al., 2014; Garny & Hendon, 2022; Wang et al., 2025). Moreover, by altering meridional and vertical temperature gradients, stratospheric ozone is also known to affect projected changes in the stratospheric and tropospheric circulation (Chiodo & Polvani, 2019; Jonsson et al., 2004), including the QBO (Butchart et al., 2023; DallaSanta et al., 2021; Tian et al., 2006), jet stream positions and strengths (Chiodo & Polvani, 2019; Haase et al., 2020; Nowack,

Abraham, et al., 2018), ENSO and the Walker circulation (Nowack et al., 2017; Nowack, Abraham, et al., 2018), Northern Atlantic Oscillation (Chiodo & Polvani, 2019; Kuroda et al., 2008), and the polar vortices (Oehrlein et al., 2020). Therefore, realistically representing the two-way coupling of ozone and climate is critical for reliable climate simulations.

However, the treatment of ozone in climate models is often internally inconsistent with the climate model state and the climate change scenario. The main reason is that interactive atmospheric chemistry schemes are typically too computationally expensive, slowing down global climate change simulations by more than a factor of two (Archibald et al., 2020; Horowitz et al., 2020). An explicit representation of ozone requires the model to calculate chemical tendencies based on complicated mathematical formulations and transport processes. As a result, only 21 out of the 60 Coupled Model Intercomparison Project Phase 6 (CMIP6) models include interactive ozone in the Diagnostic, Evaluation and Characterization of Klima (DECK) experiments (including AMIP, pre-industrial, abrupt-4×CO_2, and 1%/year CO_2 increase), despite these being among the highest-priority simulations in the CMIP framework (Masson-Delmotte et al., 2021). In particular, models without interactive ozone chemistry typically prescribe ozone ("non-interactive ozone") at fixed pre-industrial levels or as a historical climatology in abrupt-4×CO_2 runs, not including the ozone response to the abrupt-4×CO_2 forcing (Jones et al., 2011). Unlike for historical or future scenario experiments, there are also no recommended data sets for prescribing ozone concentrations in the climate sensitivity experiments within DECK, including the abrupt-4×CO_2 and 1%/year CO_2 increase experiments (Cionni et al., 2011; Hoesly et al., 2016). Moreover, among the aforementioned 21 models with interactive ozone scheme, five use the simplified linearized ozone photochemistry scheme (Linoz, McLinden et al., 2000), which is a common ozone parameterization scheme due to its low computational cost (McLinden et al., 2000). However, because of its assumptions, in particular on linearization of temperature and net chemical production (Meraner et al., 2020), it has several important limitations. These include significant bias in column ozone representation (Meraner et al., 2020), underestimation on QBO- and extratropical quasi-stationary planetary waves-related ozone variability (Meraner et al., 2020), non-applicability in the troposphere (Meraner et al., 2020), and discontinuity between polar and lower latitude regions (McLinden et al., 2000), etc.

For both efficiency and accuracy, we propose using machine learning (ML) to represent ozone interactively in climate models. As a starting point of its application, in this work, we apply this approach in climate sensitivity simulations—pre-industrial control (piCTRL) and abrupt-4×CO_2—core experiments of CMIP to characterize fundamentals in the climate response to CO_2 forcing. Nowack, Braesicke, et al. (2018) introduced an ML-based ozone parameterization that generates three-dimensional daily ozone fields for climate sensitivity simulations, using temperature as the sole input. Despite its simplicity, the scheme achieves accurate and robust offline predictions, owing to the strong connections between ozone and atmospheric temperatures described above. Nowack et al. (2019) further demonstrated the possibility to transfer the ML parameterization across climate models, subject to straightforward data transformations. This study implements this idea for the first time interactively, both in the UK Earth System Model (UKESM) and the Icosahedral Nonhydrostatic Model (ICON) climate modeling frameworks. Such an implementation introduces major challenges, in particular that the ML scheme must be able to realistically represent ozone variability and trends on long, decadal timescales when two-way coupled to the physical model state. We will demonstrate that the ML scheme allows for an interactive representation of ozone for climate sensitivity experiments, with negligible cost compared to full-chemistry schemes such as the United Kingdom Chemistry and Aerosols (UKCA) Stratosphere-Troposphere scheme (Archibald et al., 2020), by avoiding both the comprehensive computations on chemistry and transport processes. The ML parameterization is applied to both stratospheric and tropospheric ozone, though the emphasis is placed on the stratosphere, where the vast majority of atmospheric ozone resides and where ozone is known to substantially impact stratospheric dynamics (Butchart et al., 2023; Rind et al., 2014). In contrast, tropospheric ozone contributes only a small fraction of the total ozone column and has comparatively weak local radiative heating and thus limited influence on tropospheric dynamics (Andrews et al., 1987). Here we will aim to represent slower CO_2-driven tropospheric ozone trends, which can exert a significant radiative forcing under climate change (Banerjee et al., 2014; Johnson et al., 2001; Toumi et al., 1996). Previous studies have demonstrated successful applications of ML in predicting scenario-dependent ozone changes in the troposphere and stratosphere, but none have been implemented into a climate model to emulate the ozone variability associated with comprehensive ozone-related chemical mechanisms and transport processes in an online setting. For example, Mohn et al. (2023) proposed a Neural Network (NN)-based scheme for daily ozone parameterization in atmospheric models and

showed promising offline performance, but their approach is not readily adaptable for online implementation because it relies on certain catalytic chemical compounds as input—variables that cannot be obtained without running a full chemistry module or need to be specified separately as climatologies or from look-up tables. Kelp et al. (2020) trained encoder–decoder NNs to represent various chemical species from an atmospheric chemical solver offline. While this method successfully reproduced the diurnal ozone cycle with substantial computational speedup compared to traditional solvers, it exhibited numerical instability during longer-duration simulations. Other offline applications include Bayesian NN for historical ozone simulations (Sengupta et al., 2020), linear and non-linear ML techniques for future ozone projections under emission scenarios (Keeble et al., 2021). In a broader sense, ML has been gaining popularity as an optimized approach to parameterize other components in climate models in recent years, especially sub-grid processes including gravity waves (Pahlavan et al., 2024) and cloud cover (Grundner et al., 2022), and highly time-consuming components such as aerosols (Kumar et al., 2024). Overall, the application of ML approaches to stratospheric ozone research is still in its infancy. To the best of our knowledge, there has been no successful online implementation of an ML scheme for parameterizing global ozone distributions before.

In this article, we assess the effectiveness of a ML-based ozone parameterization (mloz) in reproducing (a) the temporal variability and climatological spatial distribution of ozone in idealized piCTRL and abrupt-4×CO_2 simulations, and (b) the ozone response and feedback to the quadrupling of atmospheric CO_2. The ML scheme is first implemented in UKESM and evaluated against the UKESM full chemistry module—UKCA (Archibald et al., 2020)—regarding its accuracy and efficiency. Then its transferability is assessed by applying the ML scheme trained with full chemistry data from UKESM to the ICON model.

2. Methods

2.1. The mloz Scheme

Figure 1 illustrates the mloz scheme, which uses a ML approach to parameterize ozone up to 50 km altitude. Above this altitude, a climatology from the UKESM full-chemistry simulation is applied to stabilize the upper atmospheric climate condition and to prevent instabilities caused by input-output error accumulation. The mloz represents ozone interactively, including the ozone-circulation coupling and ozone's radiative feedback. In essence, mloz uses ML to map meteorological variables from the previous timestep to the ozone volume mixing ratio at the current timestep, where we here choose daily mean time resolution. Ideally, these input variables should be independent of the chemistry module, allowing ozone prediction without solving the underlying system of coupled partial differential chemical rate equations (Pyle, 1980).

In this study, we use temperature as the only predictor because it is readily available in general circulation models that lack atmospheric chemistry components. We adopt a single column input scheme in which we consider temperatures at all vertical levels within the same column as the target ozone grid point. Temperature reflects many of the key processes that determine ozone in standard climate sensitivity simulations—including production, depletion, and transport—making it a strong predictor for ozone trends and variability, especially in the stratosphere. In the upper stratosphere, where ozone is short-lived, the production and loss processes dominating ozone variations in the region—namely Chapman photochemical and catalytic ozone loss reactions—exhibit strong temperature dependencies (Hocke & Sauvageat, 2023; Meul et al., 2014). As a result, ozone in this region is strongly anti-correlated with temperature. In the lower stratosphere, where ozone lifetimes are longer and variability is governed primarily by dynamics, ozone often varies in phase with temperature. For instance, an accelerated BDC cools the tropical lower stratosphere and enhances poleward ozone transport; the resulting temperature structure is therefore indicative of enhanced transport (Randel et al., 2021). Many aspects of ozone variabilities are also reflected in the atmospheric temperature field. The seasonal cycle of ozone—driven primarily by variations in photochemical production and large-scale circulation—is reflected in the seasonal cycle of temperature. QBO-related ozone anomalies similarly imprint on temperature variations (DallaSanta et al., 2021; Moreira et al., 2016). Long-term circulation changes that shape ozone trends under 4× CO_2 forcing are also closely tied to the magnitude of tropospheric and stratospheric warming simulated by climate models. In the troposphere, key factors controlling ozone such as humidity, precursor emissions, and convection are also correlated with temperature in piControl and abrupt-4×CO_2 scenarios, albeit more indirectly. Although these relationships are not always causal, they leave discernible imprints on the temperature field. Consequently, much

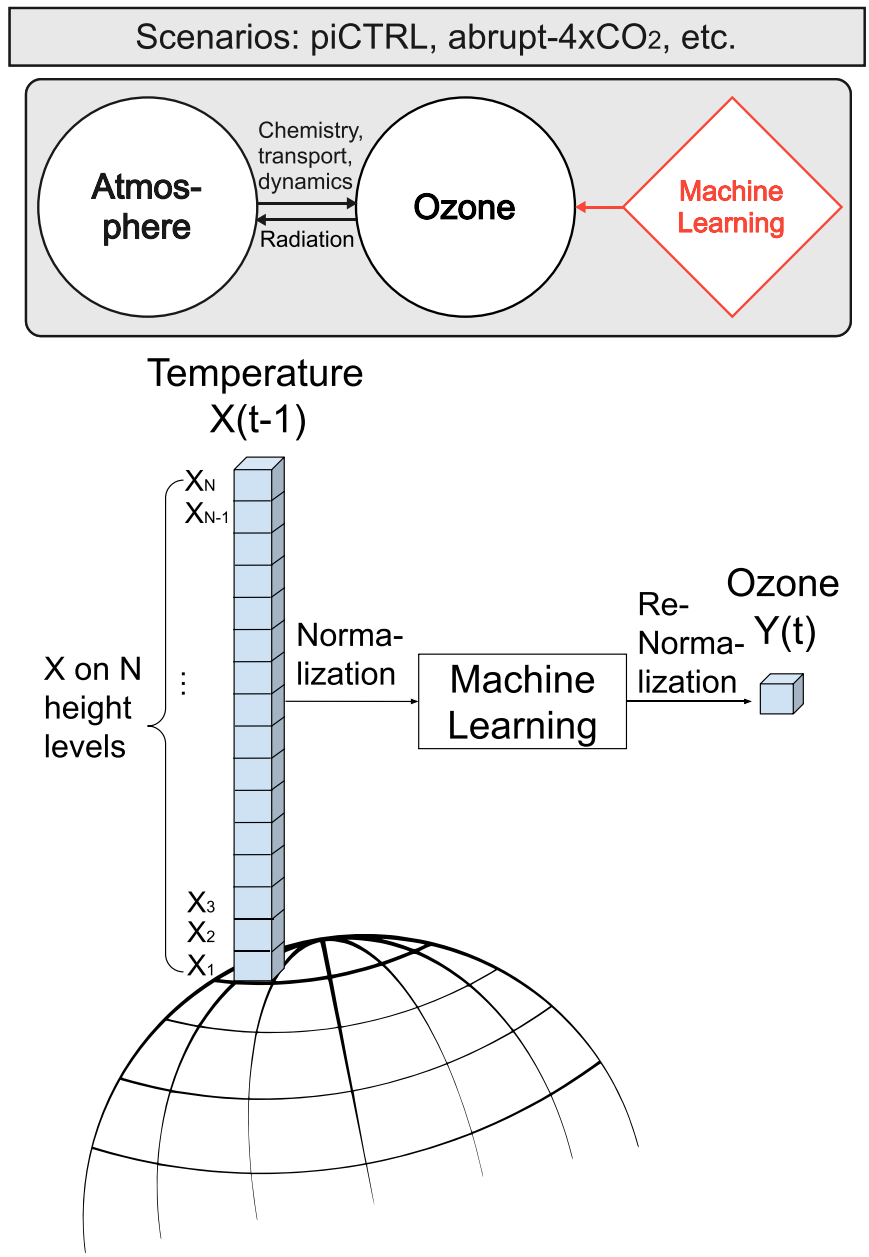

Figure 1. A schematic representation of the mloz parameterization. We use a machine learning (ML) approach to represent ozone and the associated two way climate-ozone coupling in climate models. For each ozone target grid point, we train a ML function independently for the mapping between single column temperature at timestep $t - 1$ and single point ozone at timestep t. Then the offline-trained mapping is applied for online testing in climate models. N indicates the number of vertical levels of the single column temperature input. Here $N = 76$ for the mloz in UK Earth System Model; $N = 71$ for the mloz in ICOsahedral Nonhydrostatic. Comprehensive offline comparisons showed that linear ridge regression outperforms other conventional nonlinear methods on this task. The use of column-only temperature information facilitates the parallelization on high-performance computing systems.

of the information relevant for predicting ozone—especially in the stratosphere –is embedded in the temperature profiles.

We offline tested additional predictor variables (e.g., humidity and pressure), which helped with predictive skill to a degree (Figures S1b and S1c in Supporting Information S1), but reduced online stability probably due to error accumulation stemming from the dynamic coupling between predictors and predictands. We thus favor the

temperature-only implementation here, also due to its advantages in simplicity and smaller RAM requirements. Additionally, we find that expanding the spatial extent of input features—such as using zonal or global field, can significantly enhance the offline skill (Figures S1e and S1f in Supporting Information S1), but would make parallelization on massively parallel high-performance computing systems more difficult, sacrificing some computational speed-up and portability, so that we stay with the column-wise input scheme in this paper. The ozone predictions are constrained as positive values by replacing all negative values by 0, albeit negative predictions barely appear.

Various ML methods, ranging from linear ML methods including ridge and lasso regression, to non-linear methods including Random Forests, Long Short-Term Memory and a variety of other types of NNs, have been evaluated and also previously reported (Nowack, Braesicke, et al., 2018; Nowack et al., 2019). We also ran several hackathon events with more than 100 participants to consolidate the evaluations. Despite their higher model capacities, non-linear approaches did not outperform ridge regression offline. Only in ensemble models with ridge regression as baseline model could superior performance be achieved, but such approaches would disproportionally affect runtime performance given relatively small gains in offline accuracy. For example, our offline evaluation shows that, with the same input and output features, ridge regression performs as good as feedforward NNs in most areas of the atmosphere, and slightly outperform NNs in certain regions such as tropical stratosphere and polar lower stratosphere. (Figure S1d in Supporting Information S1). The superior performance of ridge regression can be explained by the strong linear relationship between temperature and ozone in most regions of the atmosphere (Hocke & Sauvageat, 2023; Moreira et al., 2016; Randel et al., 2021). Given its intrinsic interpretability, computational efficiency, and ease of implementation, the ridge regression approach is chosen here for the parameterization.

We use ridge regression to map the temperature in a single column to the ozone at a single target grid point (Figure 1). Ridge regression is a linear regression augmented by L2-regularization, which penalizes large coefficient values and has the advantage of addressing overfitting compared to a pure linear regression model. The strength of the regularization term is controlled by the hyperparameter α. For each target grid point over all latitudes, longitudes and height levels, the ridge coefficients (c_1 to c_N) minimize a penalized residual sum of squares:

$$J^{ridge} = \arg\min_{c} \left\{ \sum_{i=1}^{n} \left(y_i - \sum_{j=1}^{N} x_{ij}\, c_j \right)^2 + \alpha \sum_{j=1}^{N} c_j^2 \right\} \tag{1}$$

Here, x_{ij} is the normalized temperature value at the jth height level for the ith sample, y_i is the normalized ozone prediction for the same sample, and N is the number of vertical levels up to 50 km in a climate model. The parameters are validated with three-fold cross-validation. The hyperparameter α is optimized according to the averaged generalization performance on validation sets. Final coefficients are refitted on the entire data set subject to the optimal cross-validated α to make full use of all available data. In the end, these result in a 4-dimensional array of ridge coefficients, where each latitude-longitude-height grid point is associated with a coefficient series (c_1 to c_N).

The implementation and evaluation of mloz is divided into two stages:

(i) Offline Training: For each model grid point at a given latitude, longitude and vertical level, a set of ridge regression coefficients $c_j, j = 1,...,N$ and hyperparameter α are trained on 40 years of UKESM full-chemistry simulations from Experiment A and Experiment B (see Table 1 for experimental set-up), separately. During this process, scaling parameters (mean and standard deviation) for temperature and ozone are also saved for use in the online implementation.

(ii) Online Testing in ICON and UKESM: A daily prediction timestep is used, where the ozone volume mixing ratio is predicted using the previous day's mean temperature profile. Thus, the mloz calculation is performed once per model day. Pre-trained regression coefficients are read from a standard NetCDF4 file and loaded at the start of the model run. Prior to the regression computation, daily mean temperatures from model level 1 to N are standardized to unit variance. The (standardized) ozone value at each grid cell on the current day is then computed via matrix multiplication between the (standardized) temperature vector on previous day and the corresponding ridge coefficients along the vertical column: $\hat{y} = \sum_{j=1}^{N} x_j\, c_j$. Afterward, the predicted ozone

Table 1
Experimental Set-Up for the Simulations

Model	Experiment	Forcing	Ozone chemistry	Ocean	Simulation years
UKESM	A	piCTRL	Full chemistry	Interactive ocean	50
	A1		mloz		
	B	abrupt-4×CO_2	Full chemistry		
	B1		mloz		
ICON	A2	piCTRL	mloz	Prescribed SSTs climatology (last 20 years of A)	30
	A3		Linoz		
	A4		Prescribed piCTRL ozone		
	B2	abrupt-4×CO_2	mloz	Prescribed SSTs climatology (last 20 years of B)	
	B3		Linoz		
	B4		Prescribed piCTRL ozone		
	B5		Prescribed 4×CO_2 ozone		

value is re-scaled back to mixing ratio unit. This computation is parallelized across grid cell blocks to ensure efficient ozone prediction throughout the global domain.

This simple regression-based scheme makes mloz particularly computationally efficient, easily runs in most parallel model environments, and is straightforward to implement across different climate models. For the transfer into ICON, a recalibration step is applied to the temperature input during the scaling process, as described in Section 2.3.

2.2. Climate Models Setup

In the online testing stage, the trained function is first applied interactively in UKESM1 (Sellar et al., 2019) to produce daily ozone simulations. These parameterized simulations are then assessed by comparing their statistics against those from the full-chemistry UKESM runs. The UKESM includes coupled components for the atmosphere, ocean, sea ice, land surface, and atmospheric chemistry. The experiments with UKESM are configured as CMIP-like simulations. Simulations are run for 50 years to allow the model to level off toward an approximate equilibrium state in the last 20 years under 4×CO_2 forcing (Table 1). All UKESM runs start from a spun-up piCTRL equilibrium state, with 111 years of spin-up initialized from the same 1,850 initial conditions as for the UKESM1-0-LL r4i1p1f2 ensemble member used for CMIP6 (Sellar et al., 2019).

UKESM employs the UKCA (Archibald et al., 2020) module, which allows for the generation of training data for mloz from its comprehensive stratospheric-tropospheric chemistry scheme (Archibald et al., 2020). It simulates 306 reactions among 87 species, with lightning NO_x emissions parameterized following (Price & Rind, 1992) and photolysis rates computed using the FastJX scheme (Telford et al., 2013). The radiative effects of ozone are interactively coupled to the model dynamics, enabling feedbacks between atmospheric composition and climate.

The atmospheric component of UKESM is the Met Office's Unified Model with a horizontal resolution of 1.875° longitude by 1.25° latitude and 85 vertical levels extending to 85 km. Subgrid-scale features such as clouds and gravity waves are parameterized, and the version used here includes a self-contained QBO. The ocean component is based on European Modeling of the Ocean model version 3.6 (Gurvan et al., 2017), using a tripolar grid with a 2° longitude resolution and enhanced latitudinal resolution (up to 0.5°) in the tropics.

Subsequently, we apply the function in another climate model—ICON—to verify its transferability, which might open up pathways to wide applicability across climate models. The ICON experiments are configured as Atmospheric Model Intercomparison Project (AMIP)-like simulations (Niemeier et al., 2023), using the configuration of ICON 2024.07 release (Müller et al., 2025), with the atmospheric component ICON-NWP (Zängl et al., 2015) coupled with the land component JSBACH 4. The ICON simulations are implemented with prescribed monthly climatological sea surface temperature and sea ice concentration derived from the last 20 years of UKESM full chemistry simulations (Table 1).

In this study, we compare mloz with Linoz and assess ozone responses to abrupt-4×CO_2 forcing by evaluating against simulations with prescribed ozone (see Table 1). ICON is run at an icosahedral resolution of R2B5, corresponding to approximately 80 km horizontal resolution. Vertically, the model includes 130 levels, extending from the surface up to around 75 km. Layer thickness increases with altitude, ranging from about 10 m near the surface to ∼500 m at 35 km and approximately 1 km at the stratopause. This model setup is adapted for a good representation of stratospheric dynamics and transport (Niemeier et al., 2023).

2.3. Re-Grid and Recalibration for the Transfer

Transferring mloz from UKESM to ICON requires regridding and recalibration due to differences in vertical coordinate systems and climatological states. Before the ML calculation, temperature inputs are interpolated onto the UKESM height levels primarily using cubic spline interpolation. Afterward, the ozone fields are bilinearly interpolated back onto ICON's vertical grid. These interpolation weights are computed once at the beginning of the model run to minimize computational overhead. To avoid extrapolation errors, particularly in regions where ICON's Earth surface definition lies under UKESM's, the lowest six ICON levels (below 270 m) are filled with climatological ozone values from UKESM full chemistry. Additionally, to mitigate the inevitable differences in temperature and ozone fields between two models, a simple recalibration is applied during the standardization step in ICON, as described in Equation 2 (Nowack et al., 2019).

$$\begin{aligned} X^{*}_{ICON} &= \left(X_{ICON} - \overline{X}_{ICON}\right)/X^{std}_{ICON} \\ Y_{ICON} &= \hat{Y}^{*}_{ICON} \times Y^{std}_{UKESM} + \overline{Y}_{UKESM} \end{aligned} \tag{2}$$

Here X, Y represent temperature and ozone, respectively. $\overline{X}_{ICON}$ and X^{std}_{ICON} are the climatology and standard deviation of temperature from the ICON run prescribed by SSTs and ozone from UKESM. By substracting $\overline{X}_{ICON}$ from X_{ICON}, the ICON temperature is recalibrated into an approximately zero mean (for piCTRL runs). The Y^{std}_{UKESM} and $\overline{Y}_{UKESM}$ are obtained from UKESM training data sets. Interestingly, we find that temperature scalings used for the transfer recalibration from piCTRL are applicable to the 4×CO_2 run.

3. Results

3.1. Online Performance in Multi-Decadal Pre-Industrial Simulations

An important baseline performance test for any parameterization is its capability to produce reasonable internal variability on daily to decadal timescales. For this purpose, the benchmark experiments in climate modeling is piCTRL simulations, that is, runs without anthropogenic influences and an assumed constant CO_2 concentration (ca. 280 ppmv). A summary of the model experiments in this study is shown in Table 1. We run UKESM with the mloz parameterization for CMIP-like simulations and compare the results with those obtained using the full UKCA chemistry scheme, assessing how well mloz captures variability and grid point-wise distributions of ozone.

Overall, mloz produces stable ozone predictions over 50 years and captures all major aspects of variability, as illustrated by four randomly selected grid-point-wise time series in Figures 2a–2d. Stable ozone output indicates that biases do not accumulate throughout the model run; otherwise, the ozone volume mixing ratios would deviate from climatology and induce increasing biases in the temperature background through feedback processes. mloz can easily reproduce seasonal variability across different atmospheric regions (Figures 2a–2d) and captures QBO-related quasi-biennial variability in the low-mid stratosphere (Figures 2b and 2c). The QBO, alternating easterlies and westerlies in the tropical stratosphere, dominates the interannual variability of tropical stratospheric ozone (Tian et al., 2006). In contrast, the prescribed ozone climatology (gray lines in Figure 2)—commonly used in climate sensitivity simulations by models without interactive chemistry—cannot represent QBO-related variability and ozone changes in response to increasing CO_2 forcing. We underline that a perfect match in internal variabilities, particularly maintaining the same phase between mloz and the full chemistry module cannot be expected in a free-running simulation, as the memory of initial conditions typically dissipates after a few weeks in the atmosphere (Kay et al., 2015; Ma et al., 2022). Nevertheless, their statistical characteristics—such as climatologies, probability density functions (PDFs), and standard deviations—can still be meaningfully compared on sufficiently large sample sizes.

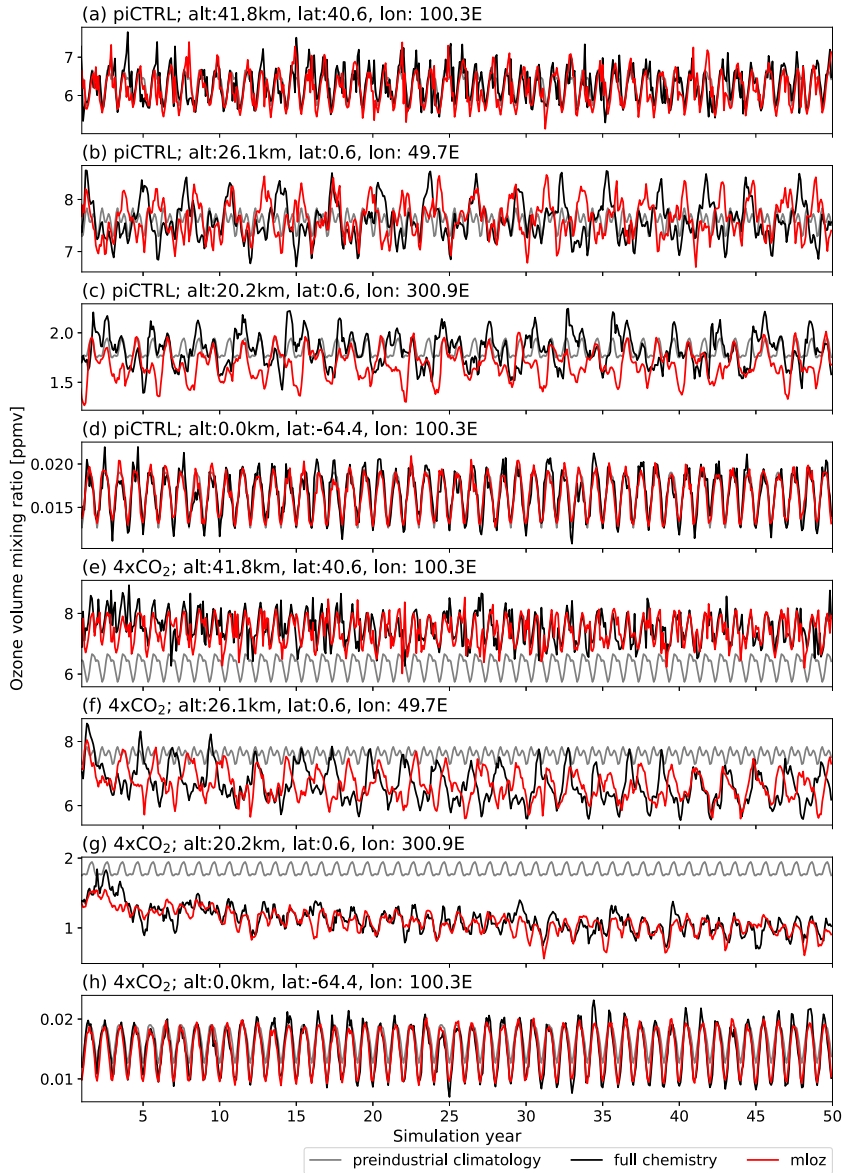

Figure 2. UK Earth System Model (UKESM) time series of mloz predictions on randomly sampled, but representatively selected grid points. Red lines show mloz-predicted ozone, black lines represent full-chemistry ozone from UKESM, and gray lines indicate the fixed preindustrial climatology from UKESM's full-chemistry simulation (Experiment A). For clarity, all time series shown are averaged to monthly means. Black/red lines in (a)–(d) are from Experiment A/A1 piCTRL simulations and those in (e)–(h) are from Experiment B/B1 4×CO_2 simulations. Ozone values are provided in ppmv. Note that the ozone time series on selected points in (b), (c), (f), and (g) depict QBO-related variability and mloz successfully captures the quasi-biennial variability in ozone, though not in-phase due to the nature of a free running climate model. The gray lines illustrate the ozone scheme that climate models without a chemistry module commonly adopt for climate sensitivity simulations —prescribed ozone at a fixed preindustrial annual climatology. The ozone output in the 1-year spin-up period is not shown in the plot.

As shown in the plot of PDF distributions of ozone from mloz compared with full chemistry at these representative points (Figure 3), mloz generally represents the stratospheric ozone distributions well. This good match in PDF distributions between mloz and full chemistry scheme not only exist on these grid points, but also across the stratosphere, as can be seen from the distributions for ozone predictions across the lower and middle stratosphere (Figure S2 in Supporting Information S1). As expected, the tropospheric ozone variability is harder to capture (Figure 3d), given limited predictability one day in advance and given the more complex ozone chemistry involved. Many key drivers of tropospheric ozone—such as lightning, which triggers ozone production by

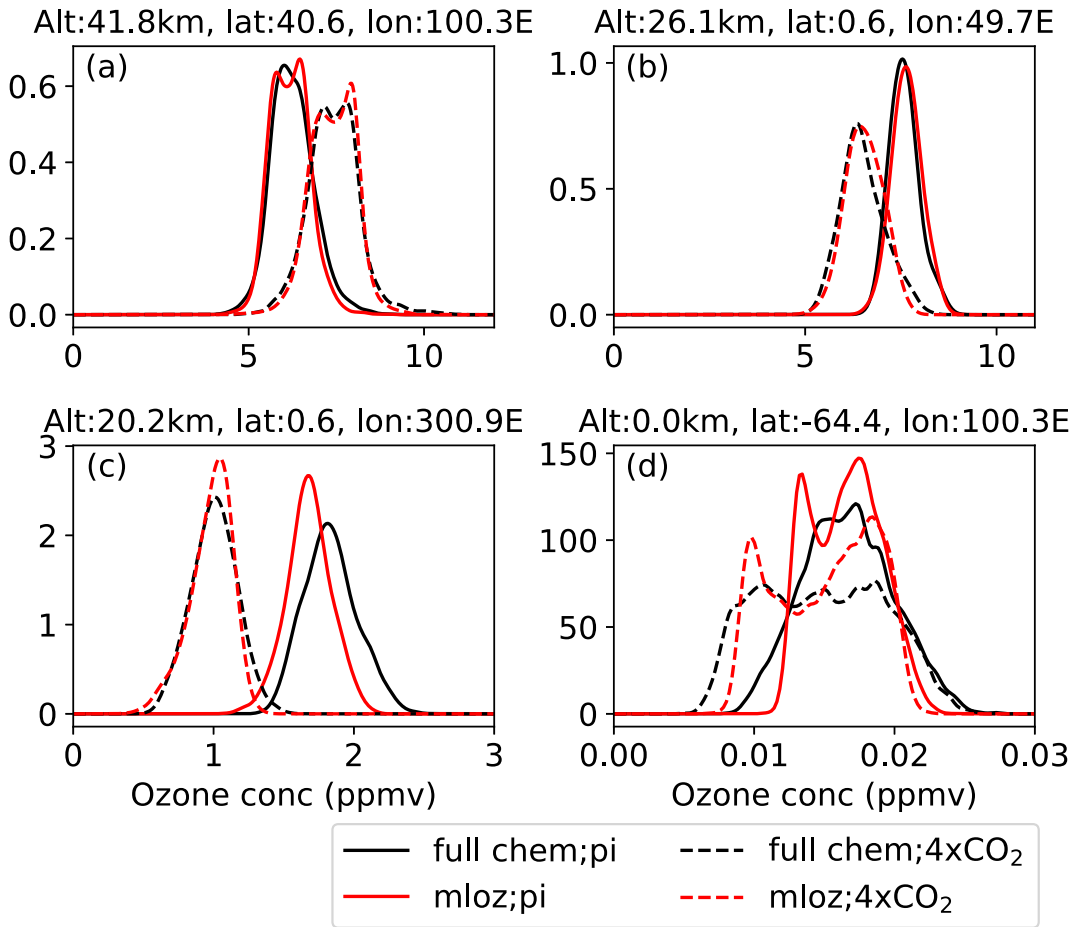

Figure 3. Probability density function (PDF) distributions of mloz ozone predictions from UK Earth System Model (UKESM) on the same grid points as in Figure 2. Red and black lines correspond to mloz and full chemistry simulations from UKESM, respectively. Solid and dashed lines denote the piCTRL and 4×CO_2 experiment, respectively. The PDFs are derived using Gaussian kernel density estimation, with the bandwidth set to 2% of the average piCTRL UKESM full-chemistry ozone value at each grid point.

initiating NO_x emissions in the troposphere (Verma et al., 2021)—are difficult to forecast one day ahead. As a result, mloz substantially underestimates the amplitude of ozone variability in the troposphere (Figure S3 in Supporting Information S1). Nonetheless, ozone variability (rather than climate trends) in the troposphere is less important compared to the stratosphere after all, due to its significantly lower concentrations and its relatively minor influence on the tropospheric circulation (Chiodo & Polvani, 2019; DallaSanta et al., 2021; Monks et al., 2015). In contrast, stratospheric ozone variability is more predictable and more accurately represented by the ML scheme (e.g., Figure S1a in Supporting Information S1). The stratosphere is less influenced by high-frequency weather systems and is more affected by the highly predictable insolation and slowly moving circulation patterns, such as the BDC and QBO. As a result, variability is generally well reproduced in the stratosphere. Some regions, however, remain challenging: in the mid-latitude stratosphere above the active wave-breaking zone, ozone variability is not fully captured by the ML scheme, either offline (R^2 fields in Figure S1a in Supporting Information S1) or online (amplitude biases in Figure S3a in Supporting Information S1). This might be due to wave-breaking leading to more non-linear relationships between ozone and temperature in those regions. Alternative architectures—with different input variables, spatial domains, or ML methods—show similarly reduced skill here (Figure S1 in Supporting Information S1), underscoring the fundamental difficulty of predicting ozone in this dynamically complex region.

In addition to accurately capturing grid-point-wise variability, the mloz scheme effectively reproduces spatial distributions of ozone, including both zonal and horizontal patterns. Above all, any ozone parameterization

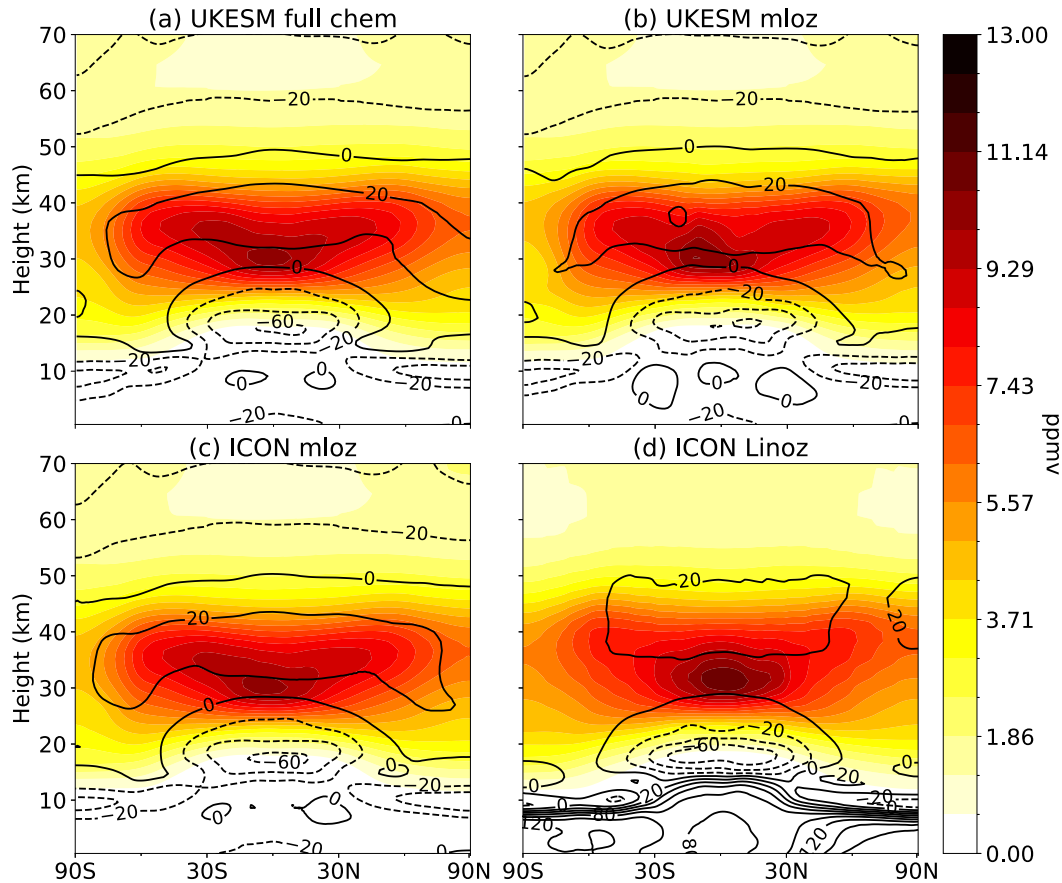

Figure 4. Zonal mean ozone climatologies from different schemes. Colors show ozone climatologies in volume mixing ratios (ppmv), and contours indicate percentage changes in the ozone climatologies in response to $4\times CO_2$. Contour intervals are 20%, with solid lines for positive changes and dashed lines for negative changes. Panel (a) shows UK Earth System Model (UKESM) full chemistry, with colors from Experiment A and contours calculated as Experiment B minus A; panel (b) shows UKESM mloz, with colors from Experiment A1 and contours from Experiment B1 minus A1; panel (c) shows ICOsahedral Nonhydrostatic (ICON) mloz, with colors from Experiment A2 and contours from Experiment B2 minus A2; and panel (d) shows ICON Linoz, with colors from Experiment A3 and contours from Experiment B3 minus A3. Note that Linoz table used in this paper is not generated from UKESM simulations so Linoz and mloz are not fully comparable. UKESM climatologies are averages over the last 20 years of interactive-ocean experiments, while ICON climatologies are 30-year means from prescribed-SST experiments; all fields are zonal means.

should be able to reproduce the long-term climatology of an interactive chemistry module with high fidelity. Figure 5a shows the percentage differences in ozone volume mixing ratios between mloz and the full chemistry module in UKESM piCTRL simulations, averaged over the final 20 years of each simulation. The bias in the ozone climatology produced by mloz is within 10% throughout the stratosphere, which is much smaller than the spread in ozone climatologies found across, for example, CMIP6 models (Keeble et al., 2021). A significant positive bias occurs between 10°S and 20°S in the middle stratosphere, indicating a slight asymmetry with the peak tilting toward the Southern Hemisphere. Notably, the bias is substantially smaller in the offline ozone prediction by mloz using the same ridge parameters (Figure S4a in Supporting Information S1). This highlights a broader characteristic of ML-based parameterizations, consistent with previous studies: their online performance cannot be reliably inferred from offline metrics alone (i.e., Mansfield & Sheshadri, 2024). Online training might help in this case, but can be slow, prone to systematic bias (Kelp et al., 2022), and such parameterizations cannot simply be learned from offline data only and transferred across climate models. Still, ideas for online training could be attempted as part of future research. In the upper troposphere, the mloz generally exhibits larger percentage deviations in ozone climatology (Figure 5a), associated with negative background temperature bias in this region (Figure S7 in Supporting Information S1). The percentage bias in the troposphere is also notably larger than in the stratosphere, reflecting reduced model skill in this region. Nevertheless, the ozone concentrations have

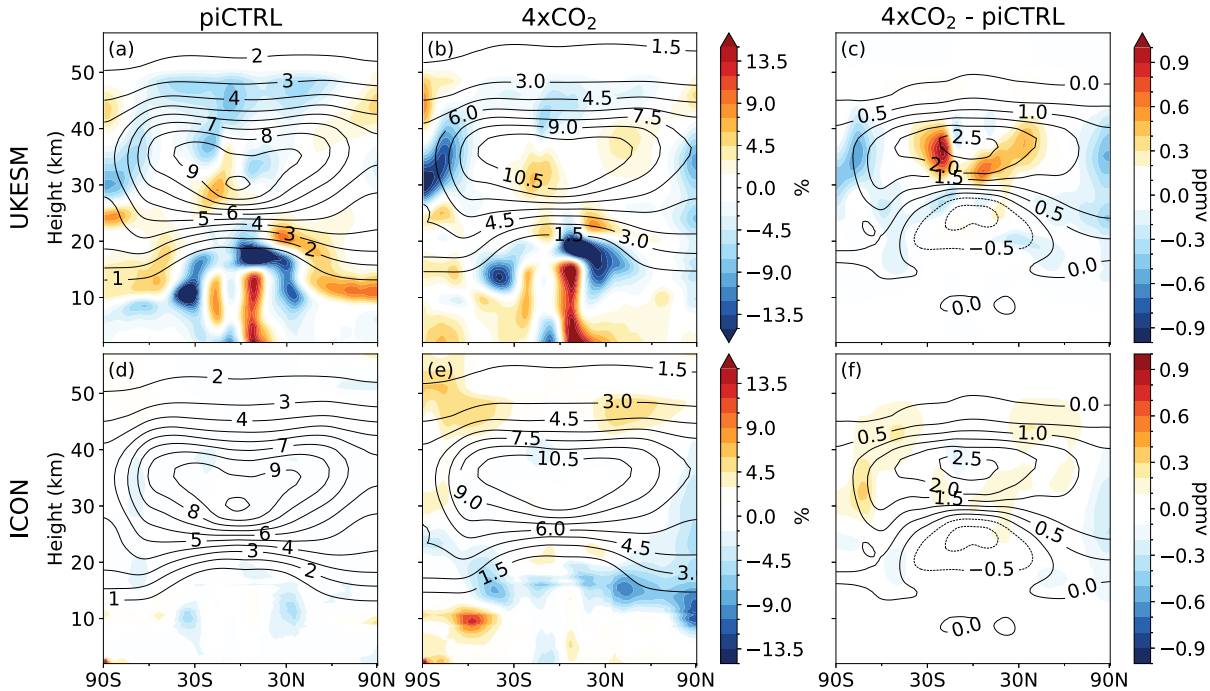

Figure 5. Long-term bias in ozone from mloz. Colors in the first two columns are the percentage differences in ozone climatology between mloz and the full chemistry simulation, specifically, Experiment A1 versus Experiment A in (a), Experiment B1 versus Experiment B in (b), Experiment A2 versus Experiment A in (d), and Experiment B2 versus Experiment B in (e). Colors in the third column are the volume mixing ratio differences between the ozone response with mloz and the ozone response with full chemistry to 4×CO_2. Contour lines indicate the UKESM full chemistry ozone, with lines in the first, second, and third column corresponding to Experiment A, Experiment B, Experiment B minus Experiment A, respectively. The UKESM ozone climatologies are averages over the last 20 years of the interactive-ocean simulations, and the ICOsahedral Nonhydrostatic climatologies are averages over the 30 years of prescribed SSTs simulations. All fields presented are zonal means.

small absolute values in the troposphere (Figures 2d and 3d), so that even small absolute deviations can result in relatively large percentage differences (Figure 5a). Finally, we demonstrate that mloz also faithfully reproduces the horizontal pattern of column ozone—the amount of ozone contained in a vertical column of the atmosphere within a unit area (Figure 6a). This is an important quantity of the atmosphere in general and resembles conservation quantities such as energy, water, and momentum used for the evaluation of ESMs. It is also of central importance for ultraviolet exposure at Earth's surface and thus a central quantity in the chemistry-climate modeling community. The long-term climatological bias in column ozone from mloz is within ±7.5% globally (Figure 6a), demonstrating superior performance compared to other simplified linearized ozone schemes which exhibit biases up to 10% (i.e., Meraner et al., 2020). This performance is also favorable when compared to the significant uncertainty among CMIP6 models, which show a spread exceeding 15% (Keeble et al., 2021).

3.2. Transferability From UKESM to ICON

Given the lack of interactive chemistry schemes in the majority of global climate models (Masson-Delmotte et al., 2021), we identify the potential to build more widely applicable ozone parameterizations as an important challenge. In particular, any such parameterization should run stably when applied across different climate models, and be easily adaptable to each model's specific climate state. Here, we explore the possibility of transferring the mloz parameterization trained on a climate-chemistry model (UKESM) to a model without a full chemistry module (here we take the ICON without the full chemistry component as an example), starting with an evaluation on a piCTRL simulation. To eliminate the inherent differences in the temperature climatologies and variability between UKESM and ICON, we apply a recalibration to the temperature input for mloz in ICON by standardizing the ICON temperature input with scalings from ICON (see Section 2.3). We show that, after recalibration, the ridge functions trained on UKESM data can be successfully applied to ICON. Similar to UKESM, ICON does not show any instability in ozone predictions over 30 years (Figure S5 in Supporting Information S1), and emulates an ozone climatology very close to UKESM full chemistry. Additionally, its long-

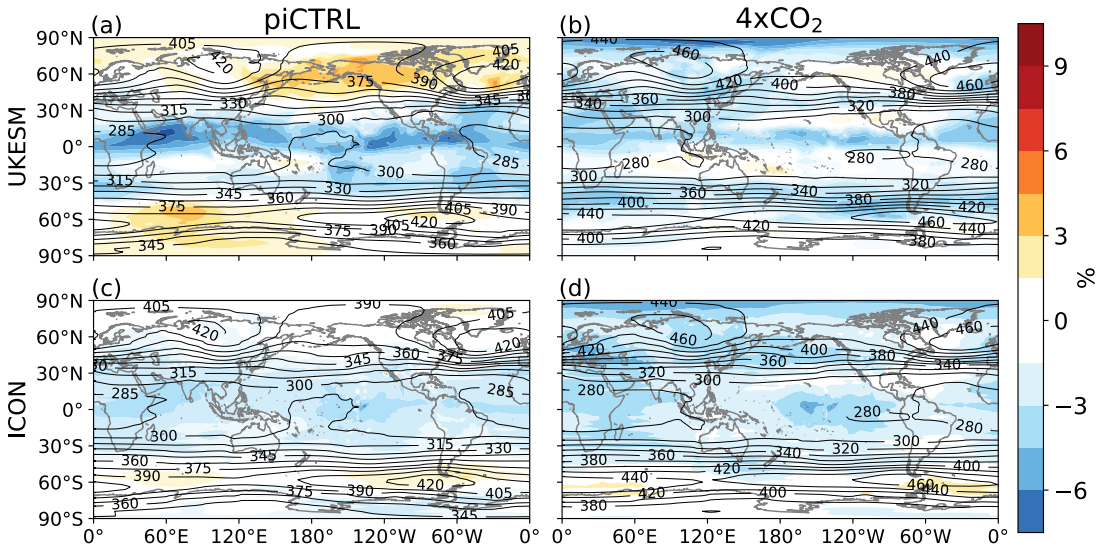

Figure 6. Long-term differences in total column ozone from mloz. Colors are the percentage differences in total column ozone climatologies between mloz and full chemistry, namely Experiment A1 minus Experiment A for (a), Experiment B1 minus Experiment B for (b), Experiment A2 minus Experiment A for (c), and Experiment B2 minus Experiment B for (d). The UKESM column ozone climatologies are averages over the last 20 years of the interactive-ocean simulations, and the ICOsahedral Nonhydrostatic climatologies are averages over the 30 years of prescribed SSTs simulations. Contours are total column ozone climatologies of UKESM full chemistry simulations in Dobson units. Only ozone concentrations below 50 km are included in the calculation of total column ozone.

term errors in both zonal and horizontal distributions relative to UKESM full chemistry ozone are minimal (Figures 5d and 6c).

Somewhat surprisingly, percentage errors in the ozone climatology in ICON with mloz compare even more favorably to the ground truth UKESM data. A possible explanation is that errors in the ozone predictions are better buffered by the ICON temperature field than by the UKESM temperature field. As shown in Figure 5d, the bias in ozone climatology from the transferred mloz is less than 2.5% in the stratosphere, and it also better reproduces tropical ozone. The bias in the troposphere is slightly higher but remains within 6%. The column ozone simulation (Figure 6c) is also better than UKESM mloz, with a bias of less than 4.5%.

3.3. Representation of Ozone Response to Abrupt-4×CO_2

Next, we evaluate the ability of mloz to capture the ozone response to climate change. With increased CO_2, ozone is expected to increase in the mid-upper stratosphere and decrease in the tropical lower stratosphere (Contour lines in Figure 4a) (Eyring et al., 2013; Keeble et al., 2017, 2021). Additionally, the acceleration of BDC under higher CO_2 enhances poleward transport of stratospheric ozone, resulting in increased ozone concentrations in the polar regions and decreased concentrations in the tropics (Randel et al., 2021). This pattern is evident in the global distribution of column ozone from UKESM full-chemistry simulations comparing piCTRL and 4× CO_2 (contour lines in Figures 6a and 6b). These changes obviously cannot be presented in simulations with fixed ozone climatologies (i.e., piCTRL ozone climatologies frequently used in abrupt-4×CO_2 CMIP runs), with important implications for the overall climate response (Jonsson et al., 2004; Nowack et al., 2015). The question is to what extent can mloz represent such responses in UKESM and ICON. Here, we train and validate a new set of ridge coefficients with UKESM abrupt-4×CO_2 full chemistry simulations over 40 years following the abrupt CO_2 increase. Note that different from piCTRL ozone, there is a centennial-millennial trend in abrupt-4×CO_2 ozone as a response to the CO_2 forcing (Nowack, Braesicke, et al., 2018). Therefore, the mloz needs to be capable of capturing the additional climate change trend in order to correctly represent the ozone climatologies over the test period (as shown in Figures 5b and 5e). The linear ML algorithm used here is good at capturing the linear climate change trend, which could also make it a better extrapolation tool than other non-linear algorithms (Nowack & Watson-Parris, 2025; Nowack, Braesicke, et al., 2018; Nowack et al., 2021).

The mloz parameterization demonstrates comparable skill in representing ozone under the abrupt-4×CO_2 scenario as in the piCTRL simulations (Figures 3, 5b, and 5e), despite the additional challenge of capturing additional

climate forcing-driven trends and the trends extending beyond the training data time horizon. Here mloz does not see the ozone trend in the final 10 years of the 50-year abrupt-4×CO_2 run (Experiment B), as the training data set covers only the first 40 years; similarly for ICON. Notably, mloz successfully reproduces these trends, as illustrated at several representative grid points (Figures 2f and 2g). This is also reflected in the good match in statistical distributions of abrupt-4×CO_2 ozone from mloz and full chemistry scheme in different regions of the atmosphere, whose averages are distinct from that of piCTRL ozone (Figures 3a–3c, Figure S2 in Supporting Information S1). The long-term bias for 4×CO_2 runs is constrained to within 10% in most of the stratosphere in UKESM (Figure 5b), and 6% in ICON (Figure 5e). However, similar to piCTRL, mloz tends to underestimate ozone amplitude in stratosphere above the mid-latitude under 4×CO_2 (Figure S3b in Supporting Information S1). This leaves room for additional developments but is within typical uncertainties in CMIP6 multi-model experiments (Keeble et al., 2021). Consistent with the good representation of 4×CO_2 ozone, mloz can also represent ozone's response to 4×CO_2 (Figures 5c and 5f), which is the difference between 4×CO_2 and piCTRL ozone. The ozone response simulated by UKESM mloz exhibits a peak bias of 0.9 ppmv in the tropical middle stratosphere (Figure 5c). However, the ozone decrease in the tropical lower stratosphere as a response to 4×CO_2, which is particularly important for ozone feedback on climate sensitivity (Nowack et al., 2015), is accurately represented by mloz (Figure 5c). This ozone decrease is primarily attributed to the acceleration of the BDC in response to 4×CO_2 and the expansion of the troposphere. For the troposphere, we cannot capture high frequency daily variability (Figures 5a and 5b), but we are able to faithfully represent forced ozone trends under changing climatic conditions (Figures 4b and 5c), which is important because of their effects on the global energy budget (Garny & Hendon, 2022; Szopa et al., 2021). The transferred mloz in ICON well represents the response of ozone to 4×CO_2, with a deviation less than 0.35 ppmv across the whole atmosphere (Figure 5f).

Horizontally, mloz effectively captures the ozone increase in polar regions and the decrease in the tropics under 4×CO_2 associated with enhanced poleward transport by the BDC (Randel et al., 2021), despite not explicitly simulating ozone transport processes. Instead, it predicts these trends based solely on local temperature information. Under 4×CO_2 forcing, the long-term bias in total column ozone from mloz remains within ±7.5% globally, with a global mean bias of only −2%. This is substantially smaller than the CMIP6 inter-model spread in global mean ozone, approximately 21% in pre-industrial and historical simulations (Keeble et al., 2021).

3.4. Representation of Ozone Feedback

Many climate modeling studies have demonstrated the importance of two-way interactions between ozone and climate change (i.e., Chiodo & Polvani, 2019; Dietmüller et al., 2014; Jonsson et al., 2004; Muthers et al., 2014; Nowack et al., 2015; Schröter et al., 2018). Stratospheric ozone modifies the climate system's response to GHG increases, impacts temperatures from the stratosphere down to the surface, and influences stratospheric and tropospheric circulation responses to the GHG forcing, thus acting as a climate feedback (Garny & Hendon, 2022). As shown in Figure 7b, the equatorial temperature response to 4×CO_2 differs in ICON if piCTRL (black solid line) or 4×CO_2 (black dashed line) ozone climatology from UKESM is prescribed. This is because ozone increases in the mid-upper stratosphere (Figure 4a) due to stratospheric cooling in response to 4×CO_2, which absorbs more solar ultraviolet radiation and mitigates local stratospheric cooling (Jonsson et al., 2004). In contrast, ozone is expected to decrease under CO_2 forcing in the tropical lower stratosphere (Figure 4a) due to self-heating effect (Meul et al., 2014). This enhances stratospheric cooling in this region. Compared with fixed ozone, including interactive ozone results in 3–5K less cooling in the upper stratosphere and enhanced cooling of 2–3K in the lower stratosphere under 4×CO_2 (comparing solid and dashed black lines), consistent with previous studies (i.e., Dacie et al., 2019). The interactive ozone configuration using the mloz scheme effectively captures this feedback in the ICON model (Figure 7b), likely due to its accurate representation of ozone responses to 4×CO_2 (Figure 5f). The strong agreement in the background temperature field for the mloz and prescribed-4×CO_2 ozone simulations is evident not only in their climatological temperature profiles (Figure 7b), but also in the middle-stratosphere temperature time series (Figure S6 in Supporting Information S1). Consequently, mloz reproduces ozone-induced feedbacks with high fidelity, maintaining long-term background temperature biases below ±1.6K throughout the troposphere and stratosphere in ICON (Figure S7f in Supporting Information S1). In UKESM, when benchmarked against full chemistry, mloz exhibits minor discrepancies in the temperature response above the equatorial region, particularly in the middle stratosphere and near the stratopause (Figure 7a) (Figure S7c in Supporting Information S1). Crucially, the close agreement in the surface temperature response between the coupled-ocean simulations from mloz and full chemistry (Figure 7a) highlights that mloz provides a

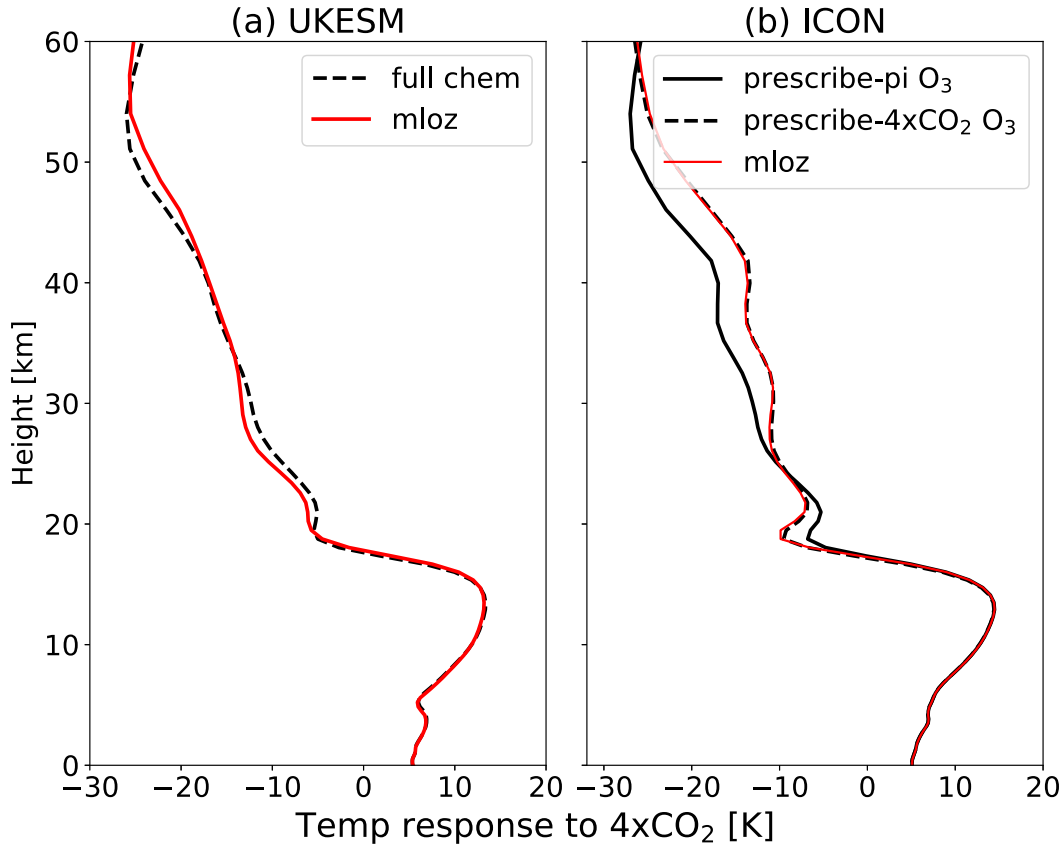

Figure 7. Profiles of equatorial temperature responses to 4×CO_2 with different ozone schemes. (a) Vertical profile of the equatorial zonal mean temperature response to 4×CO_2 from UK Earth System Model (UKESM) with mloz (red line) compared to with full chemistry (black dashed line). The temperature responses of mloz and full chemistry scheme are averaged over the last 20 years of simulations Experiment B1 minus Experiment A1 and Experiment B minus Experiment A, respectively. (b) Vertical profile of the equatorial zonal mean temperature response from ICOsahedral Nonhydrostatic (ICON) mloz (red line), with prescribed piCTRL ozone climatology from UKESM (black solid line), and with prescribed 4×CO_2 ozone climatology from UKESM (black dashed line). The discrepancy between the black solid and black dashed line indicates the bias in temperature simulation when ICON is prescribed with fixed piCTRL ozone climatology for the 4×CO_2 run. The temperature responses of mloz, prescribe-pi ozone, and prescribe-4×CO_2 ozone are averaged over the 30 years of simulations Experiment B2 minus Experiment A2, Experiment B4 minus Experiment A4, and Experiment B5 minus Experiment A4, respectively. In both panels (a) and (b), the closer the red and black dashed lines are, the more temperature modeling under CO_2 forcing benefits from mloz interactive ozone.

sufficient representation to also capture the radiative impacts of CO_2-driven ozone changes. This is important because previous studies have demonstrated that ozone feedback can significantly modulate surface warming under 4×CO_2 (i.e., Dietmüller et al., 2014; Nowack et al., 2015; Nowack, Abraham, et al., 2018). Still, using mloz in UKESM and ICON leads to a common tendency to underestimate temperatures in the tropical upper troposphere and lower stratosphere (UTLS), and to overestimate temperatures in the tropical mid-to-upper stratosphere (Figures S7a, S7b, S7d, and S7e in Supporting Information S1).

3.5. Comparison to Linoz

Given that Linoz is a standard ozone parameterization scheme in the current ICON model (Schröter et al., 2018), we here compare mloz with Linoz in ICON with respect to accuracy and efficiency. Note that since the Linoz table we use is not consistent with UKESM ozone chemistry, the UKESM full chemistry ozone cannot serve as benchmark as it is for mloz. Nevertheless, qualitative comparisons still offer valuable insights into the representation of ozone patterns and responses. As expected, there are differences between the ozone climatologies produced by mloz (which is consistent with UKESM) and Linoz, in particular in terms of peak ozone concentrations and meridional gradients (Figures 4c and 4d). The ozone time series from mloz also fluctuates more

Table 2
Average Wall-Clock Time Across All Processors for Different Chemistry Schemes

	UKESM		ICON	
Model chemistry scheme	mloz	Chemistry module	mloz	Linoz
Cores	720		912	
Length	3 months		1.5 years	
Time cost	1.75%	54.45% (Esentürk et al., 2018)	947s	2603s

Note. This table compares the computational cost of the mloz scheme with the UKCA full chemistry module in UKESM and the Linoz scheme in ICON. For UKESM, the average time cost of mloz and the chemistry module is presented as a percentage of the total runtime of a full-chemistry simulation. The time cost of the UKESM chemistry module includes contributions from chemistry, diagnostics, photolysis, convection, radiation, and dynamics within the UKCA StratTrop mechanism (Esentürk et al., 2018). For ICON, the average wall-clock time for mloz/Linoz is presented in seconds for 1.5-year AMIP-like simulations, measured by the average time differences between Experiment A2/A3 and Experiment A4.

closely around the UKESM full chemistry climatology, especially in troposphere and tropical UTLS region (Figures S5c, S5d, S5g, and S5h in Supporting Information S1). mloz closely reproduces the spatial pattern of ozone response relative to the UKESM full-chemistry simulation as shown in Figures 4a, 4c, and 5f. Linoz, on the other hand, tends to simulate a larger ozone increase in the troposphere in response to $4\times CO_2$ (contour lines in Figure 4d), consistent with the findings from previous studies with Linoz (Meraner et al., 2020). This occurs because the temperature in the troposphere rises under $4\times CO_2$ conditions, causing the linearized scheme, which depends on local temperature, to incorrectly overestimate ozone. However, it should be noted that Linoz is not specifically designed for a realistic representation of tropospheric chemistry (Meraner et al., 2020), whereas there is no such limitation on a ML ozone scheme.

Table 2 summarizes the average wall-clock time for the mloz scheme compared to the UKCA chemistry module in UKESM and the Linoz scheme in ICON. In UKESM, the full chemistry module accounts for approximately 55% of the total simulation time, with nearly half of that attributed to tracer transport processes (Esentürk et al., 2018). This means that running interactive chemistry at least doubles the UKESM model runtime. In contrast, the mloz scheme requires only 1.75% of the same simulation time, making it approximately 31 times faster than UKCA. This substantial gain in efficiency stems from bypassing the computationally intensive differential equations and transport calculations required for interactive chemistry. Instead, mloz uses only temperature as input and predicts ozone via matrix multiplication with pre-trained ridge regression coefficients. In ICON, the mloz scheme takes an average of 15.78 min for a 1.5-year AMIP-like simulation, accounting for just 2.42% of the total runtime. Compared with Linoz, mloz is still 2.75 times faster. A key difference is that mloz does not just model chemical tendencies but also replaces transport costs for chemical tracers.

4. Summary and Discussion

Over the past two decades, an increasing number of climate models have incorporated complex ozone chemistry and associated chemistry-climate coupling (Masson-Delmotte et al., 2021), which comes at a high computational cost. Still, even with today's computational capacities, comprehensive chemistry schemes remain too expensive for many modeling approaches in climate research, such as large ensembles or convection-permitting resolutions. Around two thirds of the CMIP6 models do not interactively represent ozone changes (Masson-Delmotte et al., 2021). In this context, computationally inexpensive ozone schemes that allow adaptive ozone representation are valuable tools. Here, we modeled ozone with a linear ML approach that enables fast, accurate, and stable simulations across a range of climate scenarios. The mloz scheme addresses this need by employing ridge regression to predict daily ozone concentrations based on single-column temperature inputs. We have implemented mloz in two climate models, and evaluated it for two core CMIP experiments in which most climate models still lack interactive ozone representations—piCTRL and abrupt-$4\times CO_2$.

Our work establishes the online stability of this first fully integrated ML ozone parameterization within ESMs. We have demonstrated its multi-decadal robustness and accuracy in standard climate sensitivity simulations, and the substantial speed-up compared to full complexity atmospheric chemistry simulations that it has been trained on. The mloz parameterization is around 30 times faster than the UKCA full chemistry module, and around three

times faster than Linoz. It produces stable ozone predictions over 50 years under constant forcing, and can respond interactively to a changing environment under CO_2 forcing. It well represents various aspects of ozone variability, including seasonal and QBO-related variability, despite a slight underestimation of amplitudes over the stratospheric polar regions. It produces an accurate distribution in stratospheric ozone and total column ozone, with a bias in climatology less than 10%, despite a slight asymmetry tilting toward the Southern Hemisphere above the tropics. The performance is worse in the troposphere than in the stratosphere due to the more complex ozone chemistry in the troposphere and the daily temporal resolution of mloz, targeting climate-relevant timescales rather than air pollution forecast applications. Nevertheless, our parameterization does capture long-term tropospheric ozone trends in abrupt-4×CO_2 simulations, which will contribute to overall radiative forcing of ozone. With mloz we can also realistically emulate the effect of changes in ozone on the modeled climate response under 4×CO_2 forcing (feedback), such as a reduction of upper stratospheric cooling. In that sense, mloz demonstrates strong potential for improving the fidelity of climate change projections, for example, on stratospheric and tropospheric temperature.

A central advance is that mloz is transferrable across climate models, as we have demonstrated for the successful transfer from UKESM to ICON. In a 30 years-long climate sensitivity simulation, we have tested that mloz produces a stable and highly accurate ozone representation in ICON, compared to its interactive chemistry UKESM ground truth. The bias in ozone climatologies is within 2.5% in the stratosphere, and within 6% in the most of the troposphere. We identify two main reasons for the transferability of mloz: first, the vertical temperature profiles in UKESM and ICON are consistent, especially after correcting for the climatological differences in their baseline temperature states during the re-calibration process. Second, the temperature–ozone relationship—captured by the ridge regression coefficients—remains stable across both models. These consistencies suggest that mloz can be potentially effectively applied to other climate models as well, since both the vertical temperature structure and the temperature–ozone relationship are governed by fundamental physical and chemical laws that are universally applicable across climate modeling frameworks. Therefore, models lacking a chemistry module can be equipped with a self-consistent ozone representation using mloz parameters trained on another chemistry-climate model.

One might question whether temperature alone can provide sufficient information for predicting ozone across regions. The mloz regression model derives skill from both direct and indirect relationships with temperature. In the upper stratosphere, ozone strongly anti-correlates with temperature due to the temperature dependency of photochemical and catalytic processes (Hocke & Sauvageat, 2023). For example, GHG increase (e.g., 4×CO_2) induces stratospheric cooling, which then leads to significant ozone increase in the tropical mid-upper stratosphere (Chiodo et al., 2018; Meul et al., 2014). In the lower stratosphere, where ozone has a longer lifetime and is governed primarily by dynamical processes, ozone often manifests in-phase relationship with temperature. For example, a stronger BDC leads to a colder tropical lower stratosphere and enhanced poleward ozone transport (Randel et al., 2021). A stable polar vortex, characterized by cold, isolated polar stratospheric air, hinders poleward transport of ozone across the vortex edge (Moreira et al., 2016). Seasonal and QBO-driven ozone variations are also reflected in temperature variations (DallaSanta et al., 2021; Moreira et al., 2016). These processes, though often indirect, are embedded in the temperature field, enabling the model to capture ozone variability across the atmosphere. However, in the troposphere—where ozone is influenced by emissions, humidity, and convection—daily-mean temperature alone necessarily performs poorer as a proxy, as reflected in the lower predictive skill of mloz. Including additional variables and increasing the temporal resolution will likely help, although initial online tests did not show major improvements and will also tend to lower the gain in computational efficiency. Expanding the spatial input domain beyond column-wise information improves offline performance, but is difficult to implement online in a portable way due to different parallelization strategies used in climate models. Further research is needed to refine the ML framework and address these technical challenges.

This work opens up new avenues for ML parameterizations in atmospheric chemistry and for a more consistent representation of ozone feedback across climate sensitivity simulations. Future work could for example, expand the scheme to more complex scenarios, including interactions with ozone-depleting substances and varying socioeconomic development pathways emission trajectories.

Conflict of Interest

The authors declare no conflicts of interest relevant to this study.

Availability Statement

Due to intellectual property copyright restrictions, we cannot provide the source code for the UM or JULES, used by UKESM1. The UM is available for use under license. A number of research organizations and national meteorological services use the UM in collaboration with the Met Office to undertake atmospheric process research, produce forecasts, develop the UM code and build and evaluate Earth system models. To apply for a license for the UM, go to https://www.metoffice.gov.uk/research/approach/modelling-systems/unified-model (last access: 18 March 2026), and for permission to use JULES, go to https://jules.jchmr.org (last access: 18 March 2026). ICON is available at DKRZ gitlab (https://gitlab.dkrz.de/icon/icon-model) under a permissive open source license (BSD-3C). The core Fortran modules for mloz implementation in UKESM and ICON, as well as the Python code for parameterization training, data postprocessing and visualization, are publicly available in the GitHub repository: (https://github.com/YYilingMa/machine-learning-ozone-parameterization.git) and archived at Zenodo (Ma & Abraham, 2026a). The associated training data set, trained coefficients, and online ozone predictions from mloz in UKESM and ICON are archived at Zenodo (Ma & Abraham, 2026b). Due to storage constraints, the training data and online ozone predictions are provided on a coarser grid. The original full-resolution data sets are available from Y.M. upon request.

Acknowledgments

The authors acknowledge the research funding provided by the National High-Performance Computing Center at KIT (NHR@KIT) under Grant O3PCSS, and the computing time provided on the high-performance computer HoreKa at NHR@KIT. This center is jointly supported by the Federal Ministry of Education and Research and the Ministry of Science, Research and the Arts of Baden-Württemberg, as part of the National High-Performance Computing (NHR) joint funding program (https://www.nhr-verein.de/en/our-partners). This work used Monsoon2, a collaborative High-Performance Computing facility funded by the Met Office and the Natural Environment Research Council, and JASMIN, the UK collaborative data analysis facility. This research has been supported by DWD's "Innovation Programme for Applied Researches and Developments" IAFE ICON-Seamless VH 4.7 (AS). UN got funding from the DFG research unit Volimpact (FOR 2820, Grant 398006378). We also acknowledge Sven Werchner, Pankaj Kumar, Valentin Hanft and other colleagues at KIT for their technical support in ICON. We thank the three anonymous reviewers and the editor for their insightful comments and constructive feedback, which helped to improve the clarity and quality of this manuscript. Open Access funding enabled and organized by Projekt DEAL.

References

Andrews, D. G., Leovy, C. B., & Holton, J. R. (1987). *Middle atmosphere dynamics* (Vol. 40). Academic Press.

Archibald, A. T., O'Connor, F. M., Abraham, N. L., Archer-Nicholls, S., Chipperfield, M. P., Dalvi, M., et al. (2020). Description and evaluation of the UKCA stratosphere–troposphere chemistry scheme (strattrop vn 1.0) implemented in UKESM1. *Geoscientific Model Development*, *13*(3), 1223–1266. https://doi.org/10.5194/gmd-13-1223-2020

Banerjee, A., Archibald, A. T., Maycock, A. C., Telford, P., Abraham, N. L., Yang, X., et al. (2014). Lightning NO_x, a key chemistry–climate interaction: Impacts of future climate change and consequences for tropospheric oxidising capacity. *Atmospheric Chemistry and Physics*, *14*(18), 9871–9881. https://doi.org/10.5194/acp-14-9871-2014

Benito-Barca, S., Calvo, N., & Abalos, M. (2022). Driving mechanisms for the El Niño–southern oscillation impact on stratospheric ozone. *Atmospheric Chemistry and Physics*, *22*(24), 15729–15745. https://doi.org/10.5194/acp-22-15729-2022

Butchart, N., Andrews, M. B., & Jones, C. D. (2023). Qbo phase synchronization in CMIP6 historical simulations attributed to ozone forcing. *Geophysical Research Letters*, *50*(15), e2023GL104401. https://doi.org/10.1029/2023GL104401

Chapman, S. (1930). On ozone and atomic oxygen in the upper atmosphere. *The London, Edinburgh and Dublin Philosophical Magazine and Journal of Science*, *10*(64), 369–383. https://doi.org/10.1080/14786443009461588

Chiodo, G., & Polvani, L. M. (2019). The response of the ozone layer to quadrupled CO_2 concentrations: Implications for climate. *Journal of Climate*, *32*(22), 7629–7642. https://doi.org/10.1175/JCLI-D-19-0086.1

Chiodo, G., Polvani, L. M., Marsh, D. R., Stenke, A., Ball, W., Rozanov, E., et al. (2018). The response of the ozone layer to quadrupled CO_2 concentrations. *Journal of Climate*, *31*(10), 3893–3907. https://doi.org/10.1175/JCLI-D-17-0492.1

Cionni, I., Eyring, V., Lamarque, J. F., Randel, W. J., Stevenson, D. S., Wu, F., et al. (2011). Ozone database in support of CMIP5 simulations: Results and corresponding radiative forcing. *Atmospheric Chemistry and Physics*, *11*(21), 11267–11292. https://doi.org/10.5194/acp-11-11267-2011

Dacie, S., Kluft, L., Schmidt, H., Stevens, B., Buehler, S., Nowack, P., et al. (2019). A 1D RCE study of factors affecting the tropical tropopause layer and surface climate. *Journal of Climate*, *32*(20), 6769–6782. https://doi.org/10.1175/JCLI-D-18-0778.1

DallaSanta, K., Orbe, C., Rind, D., Nazarenko, L., & Jonas, J. (2021). Dynamical and trace gas responses of the quasi-biennial oscillation to increased CO_2. *Journal of Geophysical Research: Atmospheres*, *126*(6), e2020JD034151. https://doi.org/10.1029/2020JD034151

Dietmüller, S., Ponater, M., & Sausen, R. (2014). Interactive ozone induces a negative feedback in CO_2-driven climate change simulations. *Journal of Geophysical Research: Atmospheres*, *119*(4), 1796–1805. https://doi.org/10.1002/2013JD020575

Donzelli, G., & Suarez-Varela, M. M. (2024). Tropospheric ozone: A critical review of the literature on emissions, exposure, and health effects. *Atmosphere*, *15*(7), 779. https://doi.org/10.3390/atmos15070779

Esentürk, E., Abraham, N. L., Archer-Nicholls, S., Mitsakou, C., Griffiths, P., Archibald, A., & Pyle, J. (2018). Quasi-newton methods for atmospheric chemistry simulations: Implementation in UKCA UM vn10.8. *Geoscientific Model Development*, *11*(8), 3089–3108. https://doi.org/10.5194/gmd-11-3089-2018

Eyring, V., Arblaster, J. M., Cionni, I., Sedláček, J., Perlwitz, J., Young, P. J., et al. (2013). Long-term ozone changes and associated climate impacts in CMIP5 simulations. *Journal of Geophysical Research: Atmospheres*, *118*(10), 5029–5060. https://doi.org/10.1002/jgrd.50316

Fu, Q., Solomon, S., Pahlavan, H. A., & Lin, P. (2019). Observed changes in Brewer–Dobson circulation for 1980–2018. *Environmental Research Letters*, *14*(11), 114026. https://doi.org/10.1088/1748-9326/ab4de7

Garny, H., & Hendon, H. (2022). Stratospheric ozone changes and climate. In A. H. Butler & A. Maycock (Eds.), *Scientific assessment of ozone depletion: 2022* (pp. 1–509). World Meteorological Organization.

Grundner, A., Beucler, T., Gentine, P., Iglesias-Suarez, F., Giorgetta, M. A., & Eyring, V. (2022). Deep learning based cloud cover parameterization for icon. *Journal of Advances in Modeling Earth Systems*, *14*(12), e2021MS002959. https://doi.org/10.1029/2021ms002959

Gurvan, M., Bourdallé-Badie, R., Bouttier, P.-A., Bricaud, C., Bruciaferri, D., Calvert, D., et al. (2017). Nemo ocean engine. *Zenodo*. https://doi.org/10.5281/zenodo.1472492

Haase, S., Fricke, J., Kruschke, T., Wahl, S., & Matthes, K. (2020). Sensitivity of the southern hemisphere circumpolar jet response to Antarctic ozone depletion: Prescribed versus interactive chemistry. *Atmospheric Chemistry and Physics*, *20*(22), 14043–14061. https://doi.org/10.5194/acp-20-14043-2020

Haigh, J. D. (1994). The role of stratospheric ozone in modulating the solar radiative forcing of climate. *Nature*, *370*(6490), 544–546. https://doi.org/10.1038/370544a0

Haigh, J. D., & Pyle, J. A. (1982). Ozone perturbation experiments in a two-dimensional circulation model. *Quarterly Journal of the Royal Meteorological Society*, *108*(457), 551–574. https://doi.org/10.1002/qj.49710845705

Hocke, K., & Sauvageat, E. (2023). Frequency dependence of the correlation between ozone and temperature oscillations in the middle atmosphere. *Atmosphere*, *14*(9), 1436. https://doi.org/10.3390/atmos14091436

Hoesly, R., Smith, S., Feng, L., Klimont, Z., Janssens-Maenhout, G., Pitkanen, T., et al. (2016). *input4mips.cmip6.cmip.pnnl-jgcri*. Earth System Grid Federation. https://doi.org/10.22033/ESGF/input4MIPs.10450

Horowitz, L. W., Naik, V., Paulot, F., Ginoux, P. A., Dunne, J. P., Mao, J., et al. (2020). The GFDL global atmospheric chemistry-climate model am4.1: Model description and simulation characteristics. *Journal of Advances in Modeling Earth Systems*, *12*(10), e2019MS002032. https://doi.org/10.1029/2019ms002032

Johnson, C. E., Stevenson, D. S., Collins, W. J., & Derwent, R. G. (2001). Role of climate feedback on methane and ozone studied with a coupled ocean-atmosphere-chemistry model. *Geophysical Research Letters*, *28*(9), 1723–1726. https://doi.org/10.1029/2000GL011996

Jones, C. D., Hughes, J. K., Bellouin, N., Hardiman, S. C., Jones, G. S., Knight, J., et al. (2011). The HADGEM2-ES implementation of CMIP5 centennial simulations. *Geoscientific Model Development*, *4*(3), 543–570. https://doi.org/10.5194/gmd-4-543-2011

Jonsson, A., De Grandpre, J., Fomichev, V., McConnell, J., & Beagley, S. (2004). Doubled CO_2-induced cooling in the middle atmosphere: Photochemical analysis of the ozone radiative feedback. *Journal of Geophysical Research*, *109*(D24), D24103. https://doi.org/10.1029/2004jd005093

Kay, J. E., Deser, C., Phillips, A., Mai, A., Hannay, C., Strand, G., et al. (2015). The community earth system model (CESM) large ensemble project: A community resource for studying climate change in the presence of internal climate variability. *Bulletin of the American Meteorological Society*, *96*(8), 1333–1349. https://doi.org/10.1175/bams-d-13-00255.1

Keeble, J., Bednarz, E. M., Banerjee, A., Abraham, N. L., Harris, N. R., Maycock, A. C., & Pyle, J. A. (2017). Diagnosing the radiative and chemical contributions to future changes in tropical column ozone with the um-UKCA chemistry–climate model. *Atmospheric Chemistry and Physics*, *17*(22), 13801–13818. https://doi.org/10.5194/acp-17-13801-2017

Keeble, J., Hassler, B., Banerjee, A., Checa-Garcia, R., Chiodo, G., Davis, S., et al. (2021). Evaluating stratospheric ozone and water vapour changes in CMIP6 models from 1850 to 2100. *Atmospheric Chemistry and Physics*, *21*(6), 5015–5061. https://doi.org/10.5194/acp-21-5015-2021

Kelp, M. M., Jacob, D. J., Kutz, J. N., Marshall, J. D., & Tessum, C. W. (2020). Toward stable, general machine-learned models of the atmospheric chemical system. *Journal of Geophysical Research: Atmospheres*, *125*(23), e2020JD032759. https://doi.org/10.1029/2020JD032759

Kelp, M. M., Jacob, D. J., Lin, H., & Sulprizio, M. P. (2022). An online-learned neural network chemical solver for stable long-term global simulations of atmospheric chemistry. *Journal of Advances in Modeling Earth Systems*, *14*(6), e2021MS002926. https://doi.org/10.1029/2021MS002926

Kumar, P., Vogel, H., Bruckert, J., Muth, L. J., & Hoshyaripour, G. A. (2024). MIEAI: A neural network for calculating optical properties of internally mixed aerosol in atmospheric models. *npj Climate and Atmospheric Science*, *7*(1), 110. https://doi.org/10.1038/s41612-024-00652-y

Kuroda, Y., Yamazaki, K., & Shibata, K. (2008). Role of ozone in the solar cycle modulation of the North Atlantic oscillation. *Journal of Geophysical Research*, *113*(D14). https://doi.org/10.1029/2007jd009336

Lary, D. (1997). Catalytic destruction of stratospheric ozone. *Journal of Geophysical Research*, *102*(D17), 21515–21526. https://doi.org/10.1029/97jd00912

Lu, X., Zhang, L., & Shen, L. (2019). Meteorology and climate influences on tropospheric ozone: A review of natural sources, chemistry, and transport patterns. *Current Pollution Reports*, *5*(4), 238–260. https://doi.org/10.1007/s40726-019-00118-3

Ma, Y., & Abraham, N. L. (2026a). Code for mloz: A highly efficient machine learning-based ozone parameterization for climate sensitivity simulations. *Zenodo*. https://doi.org/10.5281/zenodo.19076781

Ma, Y., & Abraham, N. L. (2026b). Datasets for mloz: A highly efficient machine learning-based ozone parameterization for climate sensitivity simulations. *Zenodo*. https://doi.org/10.5281/zenodo.19056391

Ma, Y., Yuan, N., Dong, T., & Dong, W. (2022). On the pacific decadal oscillation simulations in CMIP6 models: A new test-bed from climate network analysis. *Asia-Pacific Journal of Atmospheric Sciences*, *59*(1), 17–28. https://doi.org/10.1007/s13143-022-00286-1

Mansfield, L. A., & Sheshadri, A. (2024). Uncertainty quantification of a machine learning subgrid-scale parameterization for atmospheric gravity waves. *Journal of Advances in Modeling Earth Systems*, *16*(7), e2024MS004292. https://doi.org/10.1029/2024ms004292

Masson-Delmotte, V., Zhai, P., Pirani, A., Connors, S., Péan, C. S. B., Berger, S., et al. (2021). IPCC, 2021: Annex II: Models in climate change 2021: The physical science basis. Contribution of working group I to the sixth assessment report of the intergovernmental panel on climate change. In T. Maycock (Ed.), *Ipcc sixth assessment report* (pp. 2101–2107). https://doi.org/10.1017/9781009157896.016

Matsumi, Y., & Kawasaki, M. (2003). Photolysis of atmospheric ozone in the ultraviolet region. *Chemical Reviews*, *103*(12), 4767–4782. https://doi.org/10.1021/cr0205255

McLinden, C., Olsen, S., Hannegan, B., Wild, O., Prather, M., & Sundet, J. (2000). Stratospheric ozone in 3-D models: A simple chemistry and the cross-tropopause flux. *Journal of Geophysical Research*, *105*(D11), 14653–14665. https://doi.org/10.1029/2000jd900124

Meraner, K., Rast, S., & Schmidt, H. (2020). How useful is a linear ozone parameterization for global climate modeling? *Journal of Advances in Modeling Earth Systems*, *12*(4), e2019MS002003. https://doi.org/10.1029/2019ms002003

Meul, S., Langematz, U., Oberländer, S., Garny, H., & Jöckel, P. (2014). Chemical contribution to future tropical ozone change in the lower stratosphere. *Atmospheric Chemistry and Physics*, *14*(6), 2959–2971. https://doi.org/10.5194/acp-14-2959-2014

Mohn, H., Kreyling, D., Wohltmann, I., Lehmann, R., Maass, P., & Rex, M. (2023). Neural representation of the stratospheric ozone chemistry. *Environmental Data Science*, *2*, e41. https://doi.org/10.1017/eds.2023.35

Molina, M. J., & Rowland, F. S. (1974). Stratospheric sink for chlorofluoromethanes: Chlorine atom-catalysed destruction of ozone. *Nature*, *249*(5460), 810–812. https://doi.org/10.1038/249810a0

Monks, P. S., Archibald, A., Colette, A., Cooper, O., Coyle, M., Derwent, R., et al. (2015). Tropospheric ozone and its precursors from the urban to the global scale from air quality to short-lived climate forcer. *Atmospheric Chemistry and Physics*, *15*(15), 8889–8973. https://doi.org/10.5194/acp-15-8889-2015

Moreira, L., Hocke, K., Navas-Guzmán, F., Eckert, E., von Clarmann, T., & Kämpfer, N. (2016). The natural oscillations in stratospheric ozone observed by the gromos microwave radiometer at the NDACC station bern. *Atmospheric Chemistry and Physics*, *16*(16), 10455–10467. https://doi.org/10.5194/acp-16-10455-2016

Müller, W. A., Früh, B., Korn, P., Potthast, R., Baehr, J., Bettems, J.-M., et al. (2025). Icon: Toward vertically integrated model configurations for numerical weather prediction, climate predictions, and projections. *Bulletin of the American Meteorological Society*, *106*(6), E1017–E1031. https://doi.org/10.1175/BAMS-D-24-0042.1

Muthers, S., Anet, J. G., Stenke, A., Raible, C. C., Rozanov, E., Brönnimann, S., et al. (2014). The coupled atmosphere–chemistry–ocean model socol-mpiom. *Geoscientific Model Development*, *7*(5), 2157–2179. https://doi.org/10.5194/gmd-7-2157-2014

Niemeier, U., Wallis, S., Timmreck, C., van Pham, T., & von Savigny, C. (2023). How the Hunga Tonga—Hunga Ha'apai water vapor cloud impacts its transport through the stratosphere: Dynamical and radiative effects. *Geophysical Research Letters*, *50*(24), e2023GL106482. https://doi.org/10.1029/2023GL106482

Nowack, P., Abraham, L., Braesicke, P., & Pyle, J. (2018). The impact of stratospheric ozone feedbacks on climate sensitivity estimates. *Journal of Geophysical Research: Atmospheres*, *123*(9), 4630–4641. https://doi.org/10.1002/2017JD027943

Nowack, P., Abraham, L., Maycock, A., Braesicke, P., Gregory, J., Joshi, M., et al. (2015). A large ozone-circulation feedback and its implications for global warming assessments. *Nature Climate Change*, *5*(1), 41–45. https://doi.org/10.1038/nclimate2451

Nowack, P., Braesicke, P., Haigh, J., Abraham, L., Pyle, J., & Voulgarakis, A. (2018). Using machine learning to build temperature-based ozone parameterizations for climate sensitivity simulations. *Environmental Research Letters*, *13*(10), 104016. https://doi.org/10.1088/1748-9326/aae2be

Nowack, P., Braesicke, P., Luke, A., & Pyle, J. (2017). On the role of ozone feedback in the ENSO amplitude response under global warming. *Geophysical Research Letters*, *44*(8), 3858–3866. https://doi.org/10.1002/2016GL072418

Nowack, P., Konstantinovskiy, L., Gardiner, H., & Cant, J. (2021). Machine learning calibration of low-cost NO_2 and PM_{10} sensors: Non-linear algorithms and their impact on site transferability. *Atmospheric Measurement Techniques*, *14*(8), 5637–5655. https://doi.org/10.5194/amt-14-5637-2021

Nowack, P., Ong, Q. Y. E., Braesicke, P., Haigh, J. D., & Voulgarakis, A. (2019). Machine learning parameterizations for ozone: Climate model transferability. In *Paper presented at the 9th International Workshop on Climate Informatics, France, 2–4 October 2019*.

Nowack, P., & Watson-Parris, D. (2025). Opinion: Why all emergent constraints are wrong but some are useful—A machine learning perspective. *Atmospheric Chemistry and Physics*, *25*(4), 2365–2384. https://doi.org/10.5194/acp-25-2365-2025

Oehrlein, J., Chiodo, G., & Polvani, L. M. (2020). The effect of interactive ozone chemistry on weak and strong stratospheric polar vortex events. *Atmospheric Chemistry and Physics*, *20*(17), 10531–10544. https://doi.org/10.5194/acp-20-10531-2020

Pahlavan, H. A., Hassanzadeh, P., & Alexander, M. J. (2024). Explainable offline-online training of neural networks for parameterizations: A 1D gravity wave-QBO testbed in the small-data regime. *Geophysical Research Letters*, *51*(2), e2023GL106324. https://doi.org/10.1029/2023gl106324

Plumb, R. A. (2002). Stratospheric transport. *Journal of the Meteorological Society of Japanese Series II*, *80*(4B), 793–809. https://doi.org/10.2151/jmsj.80.793

Price, C., & Rind, D. (1992). A simple lightning parameterization for calculating global lightning distributions. *Journal of Geophysical Research*, *97*(D9), 9919–9933. https://doi.org/10.1029/92jd00719

Pyle, J. (1980). A calculation of the possible depletion of ozone by chlorofluorocarbons using a two-dimensional model. *Pure and Applied Geophysics*, *118*(1), 355–377. https://doi.org/10.1007/bf01586458

Randel, W. J., Wu, F., Ming, A., & Hitchcock, P. (2021). A simple model of ozone–temperature coupling in the tropical lower stratosphere. *Atmospheric Chemistry and Physics*, *21*(24), 18531–18542. https://doi.org/10.5194/acp-21-18531-2021

Ravishankara, A. R., Daniel, J. S., & Portmann, R. W. (2009). Nitrous oxide (N_2O): The dominant ozone-depleting substance emitted in the 21st century. *Science*, *326*(5949), 123–125. https://doi.org/10.1126/science.1176985

Rind, D., Jonas, J., Balachandran, N. K., Schmidt, G. A., & Lean, J. (2014). The QBO in two GISS global climate models: 1. Generation of the QBO. *Journal of Geophysical Research: Atmospheres*, *119*(14), 8798–8824. https://doi.org/10.1002/2014JD021678

Schröter, J., Rieger, D., Stassen, C., Vogel, H., Weimer, M., Werchner, S., et al. (2018). Icon-art 2.1: A flexible tracer framework and its application for composition studies in numerical weather forecasting and climate simulations. *Geoscientific Model Development*, *11*(10), 4043–4068. https://doi.org/10.5194/gmd-11-4043-2018

Sellar, A. A., Jones, C. G., Mulcahy, J. P., Tang, Y., Yool, A., Wiltshire, A., et al. (2019). UKESM1: Description and evaluation of the U.K. Earth system model. *Journal of Advances in Modeling Earth Systems*, *11*(12), 4513–4558. https://doi.org/10.1029/2019MS001739

Sengupta, U., Amos, M., Hosking, S., Rasmussen, C. E., Juniper, M., & Young, P. (2020). Ensembling geophysical models with Bayesian neural networks. In *Advances in neural information processing systems* (Vol. 33, pp. 1205–1217).

Solomon, S. (1999). Stratospheric ozone depletion: A review of concepts and history. *Reviews of Geophysics*, *37*(3), 275–316. https://doi.org/10.1029/1999RG900008

Solomon, S., Ivy, D. J., Kinnison, D., Mills, M. J., Neely, R. R., & Schmidt, A. (2016). Emergence of healing in the Antarctic ozone layer. *Science*, *353*(6296), 269–274. https://doi.org/10.1126/science.aae0061

Szopa, S., Naik, V., Adhikary, B., Berntsen, T., Collins, W., Fuzzi, S., et al. (2021). IPCC, 2021: Short-lived climate forcers in climate change 2021: The physical science basis. Contribution of working group i to the sixth assessment report of the intergovernmental panel on climate change. In Y. Kanaya, M. Prather, & N. Yassaa (Eds.), *Ipcc sixth assessment report* (pp. 817–922). https://doi.org/10.1017/9781009157896.008

Telford, P. J., Abraham, N. L., Archibald, A. T., Braesicke, P., Dalvi, M., Morgenstern, O., et al. (2013). Implementation of the Fast-JX photolysis scheme (v6.4) into the UKCA component of the MetUM chemistry-climate model (v7.3). *Geoscientific Model Development*, *6*(1), 161–177. https://doi.org/10.5194/gmd-6-161-2013

Tian, W., Chipperfield, M. P., Gray, L. J., & Zawodny, J. M. (2006). Quasi-biennial oscillation and tracer distributions in a coupled chemistry-climate model. *Journal of Geophysical Research*, *111*(D20). https://doi.org/10.1029/2005jd006871

Toumi, R., Haigh, J. D., & Law, K. S. (1996). A tropospheric ozone-lightning climate feedback. *Geophysical Research Letters*, *23*(9), 1037–1040. https://doi.org/10.1029/96GL00944

Verma, S., Yadava, P. K., Lal, D., Mall, R., Kumar, H., & Payra, S. (2021). Role of lightning NO_x in ozone formation: A review. *Pure and Applied Geophysics*, *178*(4), 1425–1443. https://doi.org/10.1007/s00024-021-02710-5

Wang, J., Chiodo, G., Ayarzagüena, B., Ball, W. T., Diallo, M., Hassler, B., et al. (2025). Exploring ozone–climate interactions in idealized CMIP6 deck experiments. *Atmospheric Chemistry and Physics*, *25*(23), 17819–17844. https://doi.org/10.5194/acp-25-17819-2025

Zängl, G., Reinert, D., Rípodas, P., & Baldauf, M. (2015). The icon (icosahedral non-hydrostatic) modelling framework of DWD and MPI-M: Description of the non-hydrostatic dynamical core. *Quarterly Journal of the Royal Meteorological Society*, *141*(687), 563–579. https://doi.org/10.1002/qj.2378

Zawodny, J. M., & McCormick, M. P. (1991). Stratospheric aerosol and gas experiment ii measurements of the quasi-biennial oscillations in ozone and nitrogen dioxide. *Journal of Geophysical Research*, *96*(D5), 9371–9377. https://doi.org/10.1029/91jd00517